

Coordinates

Volume XIX, Issue 3, March 2023

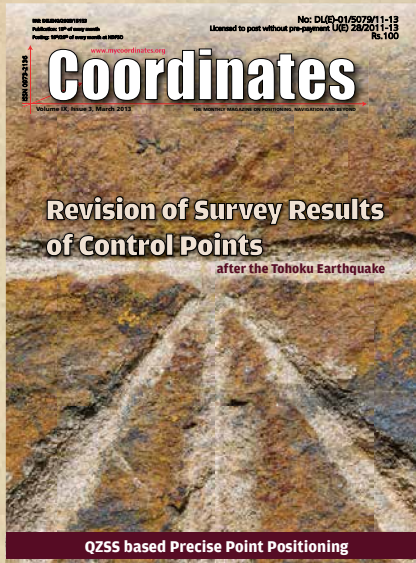
THE MONTHLY MAGAZINE ON POSITIONING, NAVIGATION AND BEYOND

GNSS-based velocity field of the African continent

**Multi-frequency GNSS Integrated Cost-effective Antenna
for Automotive Applications**

In Coordinates

10 years before...



mycoordinates.org/vol-9-issue-3-March-2013

Revision of Survey Results of control points

Atsushi YAMAGIWA and Yohei HIYAMA

Geodetic Department, Geospatial Information Authority of Japan

In order to contribute to swift restoration/ reconstruction of the disaster-stricken area, and to ensure stable provision of Survey Results for many years to come, the amount of future deformation was estimated by taking post-seismic deformation monitored by GEONET stations into account. After discussions with regard to an appropriate time for re-publication, revised Survey Results of GEONET stations were released on May 31, 2011. Precise geodetic surveys were conducted at some of triangulation stations, and Survey Results for the remaining triangulation stations were revised through calculations based on the correction parameters.

An approach to effective land registration

Hyunil Yoo and Handon Joo

Korea Cadastral Survey Corporation,
Seoul, Republic of Korea

In Turkmenistan, the government owns and manage a whole nation's land, and distribute a certain amount of land to each public in order to encourage agricultural farming and enhance productivity. As a result, land administration has focused on dealing with land information to generate reference data for taxation and national decision-making instead of securing and determining private land ownership.

QZSS LEX message data for precise point positioning

C H Wickramasinghe and L Samarakoon

aGeoinformatics Center, Asian Institute of Technology, Bangkok, Thailand

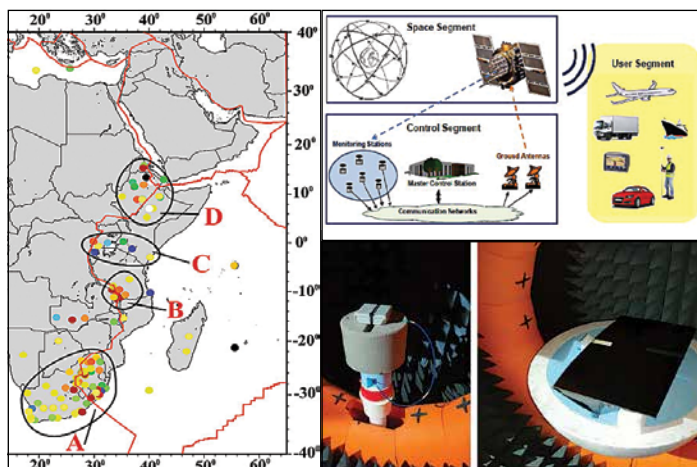
QZSS based PPP is not restricted by the limitation of GSM network such as coverage and weak signal as in the case of IGS data. Thus, QZSS PPP brings more possibility, such as real time PPP positioning in remote area such as mountains and even in the ocean.

Mitigating the systematic errors of e-GPS leveling

Lao-Sheng Lin

Associate Professor, Department of Land Economics
National Chengchi University, Taiwan

The test results show that the proposed method can mitigate the systematic errors of orthometric height from e-GPS leveling efficiently



In this issue

Coordinates Volume 19, Issue 3, March 2023

Articles

- gLAB: an advanced GNSS software for research and pedagogical purposes** ADRIÀ ROVIRA-GARCIA, DEIMOS IBÁÑEZ-SEGURA, MOWEN LI, MARÍA TERESA ALONSO, JAUME SANZ, JOSÉ MIGUEL JUAN AND GUILLERMO GONZÁLEZ-CASADO 5
- Determination of a GNSS-based velocity field of the African continent** SATURDAY E. USIFOH, BENJAMIN MÄNNEL, PIERRE SAKIC, JOSEPH D. DODO AND HARALD SCHUH 11
- MAGICA project: Crossed IFA Multi-frequency GNSS Integrated Cost-effective Antenna for Automotive Applications** MARCO ANTONIO VÉLEZ, JOSE JAVIER VICENTE, JOAN GEMIO, LAIA VILALTA, LAURA TANTINYÀ, ALBERTO GIL, ADRIÁN CARDALDA, DANIEL BAÑOS, PERE MOGAS AND JOAQUÍN REYES 19

Columns

- Old Coordinates** 2 **My Coordinates** EDITORIAL 4 **News** GIS 27 GNSS 28 IMAGING 29 UAV 30 LBS 310 INDUSTRY 32
- Mark Your Calendar** 34

This issue has been made possible by the support and good wishes of the following individuals and companies

Adrià Rovira-Garcia, Adrián Cardalda, Alberto Gil, Benjamin Männel, Daniel Baños, Deimos Ibáñez-Segura, Guillermo González-Casado, Harald Schuh, Jaume Sanz, Joan Gemio, Joaquín Reyes, José Miguel Juan, Jose Javier Vicente, Joseph D. Dodo, Laia Vilalta, Laura Tantinyà, María Teresa Alonso, Marco Antonio Vélez, Mowen Li, Pere Mogas, Pierre Sakic and Saturday E. Usifoh; SBG System, and many others.

Mailing Address

A 002, Mansara Apartments
C 9, Vasundhara Enclave
Delhi 110 096, India.
Phones +91 11 42153861, 98102 33422, 98107 24567

Email

[information] talktous@mycoordinates.org
[editorial] bal@mycoordinates.org
[advertising] sam@mycoordinates.org
[subscriptions] iwant@mycoordinates.org

Web www.mycoordinates.org

Coordinates is an initiative of CMPL that aims to broaden the scope of positioning, navigation and related technologies. CMPL does not necessarily subscribe to the views expressed by the authors in this magazine and may not be held liable for any losses caused directly or indirectly due to the information provided herein. © CMPL, 2023. Reprinting with permission is encouraged; contact the editor for details.

Annual subscription (12 issues)

[India] Rs.1,800* [Overseas] US\$100*

*Excluding postage and handling charges

Printed and published by Sanjay Malaviya on behalf of Coordinates Media Pvt Ltd

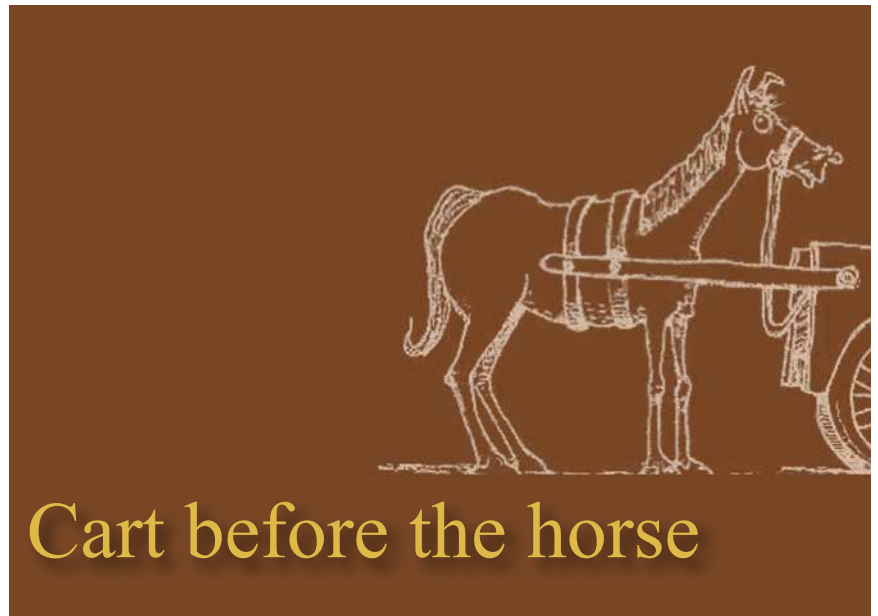
Published at A 002 Mansara Apartments, Vasundhara Enclave, Delhi 110096, India.

Printed at Thomson Press (India) Ltd, Mathura Road, Faridabad, India

Editor Bal Krishna

Owner Coordinates Media Pvt Ltd (CMPL)

This issue of Coordinates is of 36 pages, including cover.



GPT-4, Google Bard AI, Character.AI, Bing AI Chat, YouChat, ...

These growing and evolving bots,

Have already encroached the cognitive domain,

Are gearing up for a fierce battle of supremacy among themselves,

And eventually some of them,

May rein in the world of the technology,

And in due course, the humankind

Who apparently has volunteered

To vacate the driving seat.

Looks like, the technology, otherwise, an enabler,

Is set to occupy the driving seat.

Bal Krishna, Editor
bal@mycoordinates.org

ADVISORS Naser El-Sheimy PEng, CRC Professor, Department of Geomatics Engineering, The University of Calgary Canada, George Cho Professor in GIS and the Law, University of Canberra, Australia, Professor Abbas Rajabifard Director, Centre for SDI and Land Administration, University of Melbourne, Australia, Luiz Paulo Souto Fortes PhD Associate Professor, University of State of Rio Janeiro (UERJ), Brazil, John Hannah Professor, School of Surveying, University of Otago, New Zealand

gLAB: an advanced GNSS software for research and pedagogical purposes

We give an example of a straightforward procedure tailored to understand and question the effects of different error components in both SIS domain and the position domain



Adrià Rovira-Garcia
 Research group of Astronomy and Geomatics, Universitat Politècnica de Catalunya, Spain
 Corresponding author: Universitat Politecnica de Catalunya, Spain, adria.rovira@upc.edu



Guillermo González-Casado
 Research group of Astronomy and Geomatics, Universitat Politècnica de Catalunya, Spain



José Miguel Juan
 Research group of Astronomy and Geomatics, Universitat Politècnica de Catalunya, Spain



Deimos Ibáñez-Segura
 Research group of Astronomy and Geomatics, Universitat Politècnica de Catalunya, Spain



Mowen Li
 Research group of Astronomy and Geomatics, Universitat Politècnica de Catalunya, Spain



María Teresa Alonso
 Research group of Astronomy and Geomatics, Universitat Politècnica de Catalunya, Spain



Jaume Sanz
 Research group of Astronomy and Geomatics, Universitat Politècnica de Catalunya, Spain

Abstract

The Global Navigation Satellite System (GNSS) allows computing the Position, Velocity and Time (PVT) of users equipped with appropriate hardware (i.e. an antenna and a receiver) and software. The latter estimates the PVT from the ranging measurements and ephemeris transmitted by the GNSS satellites in frequencies of the L band.

The research group of Astronomy and Geomatics (gAGE) at the Universitat Politecnica de Catalunya (UPC) has been developing the GNSS LABORatory (gLAB) tool suite since 2009, in the context of the European Space Agency (ESA) educational program on satellite navigation (EDUNAV). gLAB is a multi-purpose software capable of determining the PVT in several modes: stand-alone (e.g. as a smartphone or car navigator), differential (e.g. surveying equipment or precise farming), and

augmented with integrity (e.g. civil aviation or safety of life applications).

gLAB has been designed for two main sets of users and functions. The first one is to educate University students and professionals in the art and science of GNSS data processing. This includes newcomers to the GNSS field that highly appreciate the Graphical User Interface (GUI), the default templates with the necessary configuration or the messages with warnings and errors. The second group of users are those with previous experience on GNSS. Those are interested into a high computation speed, high-accuracy positioning, batch processing and access to the intermediate computation steps.

In the present contribution, we present some examples in which gLAB serves as an education platform. The data sets are actual GNSS measurements collected by the publicly available International GNSS Service (IGS), together with other IGS products such as the satellite orbits and clocks broadcast in the navigation message. The proposed methodology and procedures are tailored to understand the effects of different error components in both the Signal in Space (SIS) and the position domain, by activating or deactivating different modeling terms in gLAB. The results illustrate some examples of how the PVT can be enhanced or deteriorated when using different processing strategies or propagation effects present in the GNSS signals traversing the atmosphere, among others.

We conclude that gLAB is a useful tool to learn GNSS data processing or to expand any prior knowledge.

Nomenclature

The mathematical symbols used in the present contribution are described in what follows:

ρ_i^j	Geometric distance, in meters, between the antennae of receiver “i” and satellite “j”
C	Speed of light, in meters/second
δT_i and δT^j	Clock offsets, in seconds, of receiver “i” and satellite “j”
f_m	Signal frequency, in Hertz
$\alpha_m = \frac{40.3 \cdot 10^{16}}{f_m^2}$	Conversion factor from Total Electron Content Units to meters of delay at the frequency
$Trop_i^j$	Slant tropospheric delay, in meters, between receiver “i” and satellite “j”
$STEC_i^j$	Slant ionospheric delay, in Total Electron Content Units, between receiver “i” and satellite “j”
DCB_i and DCB^j	Hardware delays, in meters, of receiver “i” and satellite “j”
ε_i^j	Noise, in meters, of the GNSS signal between receiver “i” and satellite “j”

Acronyms

APC	Antenna Phase Center
CA	Coarse Acquisition
DCB	Differential Code Bias
ESA	European Space Agency
FOC	Full Operational Capability
gAGE	group of Astronomy and Geomatics
gLAB	GNSS LABORATORY
GNSS	Global Navigation Satellite System
GUI	Graphical User Interface
ICA	Ionospheric Correction Algorithm
IGS	International GNSS Service
ITU	International Telecommunication Union
PVT	Position, Velocity and Time
SBAS	Satellite Based Augmentation System
STEC	Slant Total Electron Content
SIS	Signal in Space
SPS	Standard Positioning Service
TECU	Total Electron Content Unit
UPC	Universitat Politècnica de Catalunya

Introduction

The origin of navigation dates back to ancient times, when sailors computed the position and course with the use of Astronomic, Cartographic and Geometry references. The principles and techniques to guide vessels from a given origin to a destination

remained unchanged for several millennia. However, with the advent of space activities following the first artificial satellite launch Sputnik in 1957, the navigation has been revolutionised.

Global Navigation Satellite System (GNSS) [1] [2] comprises the space and ground segments that allow users equipped with appropriate hardware and software to compute its Position, Velocity and Time (PVT), see Figure 1. The space segment is composed by a constellation of space vehicles at an almost circular orbit of about 20,000 km in height [3].

Three constellations have already declared their Full Operational Capability (FOC). Namely, the Global Positioning System (GPS, US Air Force), completed in 1994; the Global Navigation Satellite System (GLONASS, Russian Federal Space Agency) completed in 1995 (and restored in 2011); BeiDou Navigation Satellite System (BDS, China National Space Administration) commissioned in 2020. The fourth constellation is being completed: the Galileo (European Commission). Together, these four GNSS constellations account for more than 100 satellites.

Each GNSS monitors the satellites by means of a worldwide network of few tens of permanent stations with ground antennas. Such control segment maintains the GNSS satellites healthy and performing nominally. The status of each GNSS constellation can be monitored in real-time at the websites [5]-[8].

The present contribution focusses on the third segment,

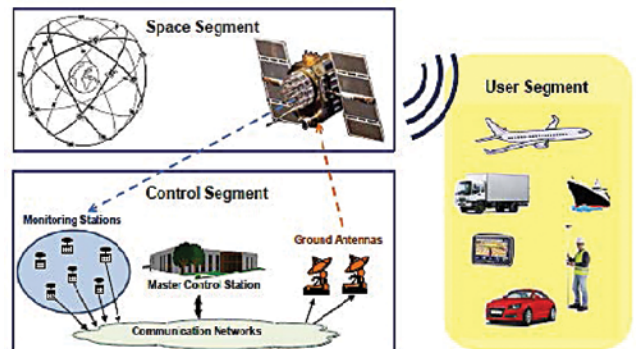


Figure 1. GNSS Architecture

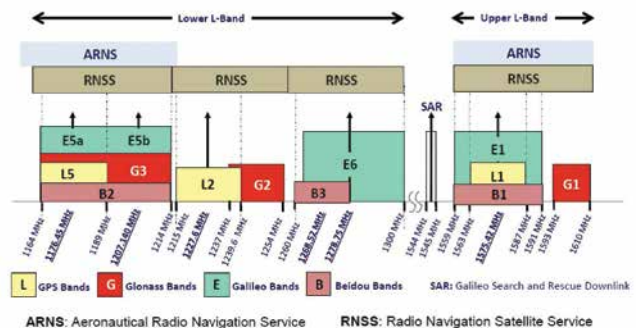


Figure 2. GPS (L), Glonass (G), Galileo (E) and Beidou (B) frequency bands.

composed by users of the GNSS. Currently, there are more than 5 billion GNSS devices in use across the world, a number expected to double by 2031 [9]. The GNSS receiver acquires and demodulates radio-navigating signals at the frequencies of the L band, i.e. around 1.2 GHz. Those frequencies are allocated by the International Telecommunication Union (ITU) [10] and are depicted in Figure 2.

The receiver then generates the code and carrier-phase measurements (i.e. the so-called observables). These measurements are used to estimate the PVT of the GNSS receiver by means of Weighted Least Squares (WLS) or the Kalman filter [11], among other techniques. Currently, several software packages exist that are capable of processing GNSS data in an automatic manner.

The GNSS LABORatory tool (gLAB) is an advanced educational multi-purpose software used for processing and analysing GNSS data [12][13]. Since 2009, gLAB has been developed by the research group of Astronomy and Geomatics (gAGE) at the Universitat Politècnica de Catalunya (UPC), in the context of several contracts with the European Space Agency (ESA).

gLAB is open-source and allows to fully control its internal processing through its many configuration options. This is a great advantage with respect to proprietary GNSS data processing programs produced by receiver manufacturers, or other entities, which do not allow any modification and hence, from the user/scientific point of view, are black boxes.

The remaining of the present contribution is organised as follows. Section 2 addresses the basic GNSS measurement equation. Section 3 presents the data used. Section 4 analyses in detail the effects of considering/neglecting some modelling terms. Last section concludes the paper summarizing the results.

Methodology

Equation 1 presents the fundamental modelling of the code pseudorange measurements, in meters, whose terms are defined in the Nomenclature section.

$$P_i^j = \rho_i^j + c(\delta T_i - \delta T^j) + Trop_i^j + \alpha_m \cdot STEC_i^j + DCB_i + DCB^j + \varepsilon_i^j$$

where the GNSS signal has propagated from the antenna of the emitting satellite to the antenna of the receiver. Without the loss of generality, but for clarity purposes, we restrict our analysis to the signals of the GPS constellation, at the frequency f_1 and for the civilian Coarse Acquisition (CA) pseudorange measurement.

The geometric distance ρ_i^j is the square root between the coordinates of the receiver (X_i, Y_i, Z_i) and those of the satellite (X^j, Y^j, Z^j) . Fortunately, we can linearize ρ_i^j using a Taylor

expansion and apply linear Algebra procedures to solve for the user position, its velocity, and its time offset δT_i with respect to GNSS time. The interested reader is pointed to [1]-[4] for further details.

gLAB implements different options to account the different model terms in Eq.1. For instance, the one defined in the Standard Positioning Service (SPS) of GPS [14], which is embedded in most of the mass-market receivers that we use in our everyday life. Figure 3 depicts the gLAB Graphical User Interface (GUI) modelling options, stored as pre-configured templates.

Hence, the gLAB user can use this baseline configuration effortlessly. It is worth to note, that these options can be modified to meet most of GNSS data processing needs, or, as we will see in the next section, the default options can be modified to get hands-on education on satellite navigation.

The gLAB GUI was designed having in mind newcomers to the GNSS field, such as our students at UPC, other Universities or professional courses where we teach GNSS. Every option displays information, so that the user can get familiar with the options that is selecting. In addition, it triggers warnings and errors to avoid any miss-configuration of the tool. Finally, it is worth to mention a second group of users with previous experience on GNSS, such as professionals and companies. Those are interested into the high computation speed offered by gLAB, its high-accuracy positioning capabilities in batch processing and access to the intermediate computation steps.

Data Set

GNSS data can be obtained free of charge from the International GNSS Service (IGS) [15][16]. Figure 4 depicts the status of the extensive permanent network of stations belonging to IGS and available from [17]. Any user can download GNSS measurements, satellite positions (i.e. ephemerides), and Earth rotation parameters, among other products.



Figure 3. Modelling tab of gLAB GUI with default options selected for the SPS.

As an example, we gathered data from a permanent station named Cachoeira Paulista (i.e. “CHPI” according to the IGS naming convention). The receiver is located in the south of Brazil, at a geographical longitude of -22.7° and latitude of -45.0° . We processed 24 h of data belonging to January 1st 2004, a year within the maximum of the 23rd Solar Cycle. The latitude and date of the experiment are chosen so that the ionospheric delay on the GNSS measurements is greatest.

Results

This section presents some examples of processing computed with the gLAB tool. The approach is tailored to understand the effect of error components in both the Signal in Space (SIS) domain and in the position domain. In order to address quantitatively and qualitatively such effects, we follow the procedure of activating or deactivating some SPS modelling terms in gLAB.



Figure 4. IGS network status on March 2022. The green circles depict operating stations, whereas red triangles indicate stations whose data is not available.

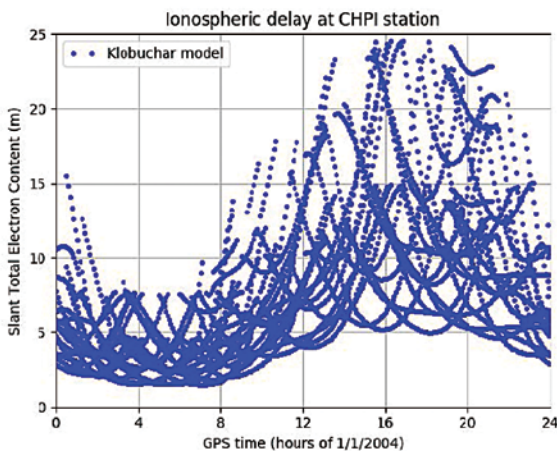


Figure 5. Ionospheric Slant Total Electron Content at permanent IGS station CHPI, modelled by Klobuchar.

Figure 5 depicts the delay occurred at the ionosphere, i.e. the upper layer of the atmosphere comprised from 60 to more than 2000 km of altitude. The electromagnetic energy from the Sun produces photoionization, which produces free electrons that interact (i.e. delaying) with the GNSS signals propagating from the GPS satellites to the receiver at CHPI.

In order to correct this delay, the SPS employs the Klobuchar model [18] as Ionospheric Correction Algorithm (ICA). The Klobuchar ICA uses eight coefficients transmitted in the navigation message that are updated every day. The Klobuchar can correct the ionospheric delay with Root Mean Square (RMS) errors between 50 to 60%.

We now turn our attention to the navigation performance. Since we are using data collected at a permanent ground station, we know its coordinates with an accuracy of few centimetres. Therefore, we can infer the navigation error of SPS modelling in Eq. 1, by computing the difference from the estimated coordinates of CHPI and those already known. For clarity purposes we will separate such differences (i.e. errors) in the vertical and horizontal planes.

Figure 6 depicts the effect of correctly modelling the ionospheric delay on the user coordinates. For this purpose, the process is

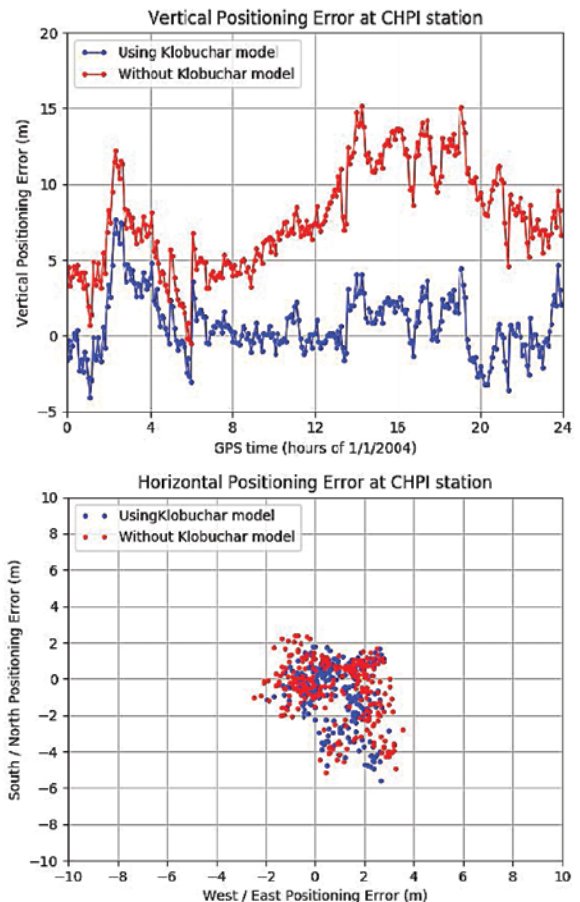


Figure 6. Vertical (top) and Horizontal (bottom) errors obtained with (blue) and without (red) Klobuchar model.

executed twice. In the first run (whose results are depicted in blue colour), we apply the full SPS modelling, with all terms of Eq.1 included. In the second run (depicted in red colour), we intentionally disconnect the ionospheric model, maintaining all other processing options from the SPS unchanged.

We can observe that the vertical component of the error is degraded by a factor three when the ionospheric delay is not corrected. As it can be seen, the vertical position error is linked to the ionospheric delay modelling previously depicted in Figure 5. The bottom plot depicts the horizontal component of the error, by plotting the North vs the East error. In this case, we do not appreciate a degradation of the error.

The reason for such asymmetry in the vertical and horizontal is an example of question posed to the students using gLAB in the laboratory sessions. The analysis of the results raises interesting questions and discussions that link the observed results with the theoretical aspects seen in the lectures.

Conclusions

gLAB is a useful tool to learn about GNSS data processing or to expand any prior knowledge. Using actual data sets collected by the publicly available IGS network, we give an example of a straightforward procedure tailored to understand and question the effects of different error components in both SIS domain and the position domain. The gLAB tool suite can be downloaded together with different Books and Tutorials on GNSS Data Processing from our website gauge.upc.edu.

Acknowledgements

The present work was supported in part by the project RTI2018-094295-B-I00 from the Agencia Española de Investigación of the Spanish Ministry of Science, Innovation and Universities

MCIN/AEI 10.13039/50110001103, which is co-founded by the FEDER program. The authors acknowledge the use of data and products provided by the International GNSS Service.

References

- [1] Parkinson B, Spilker J, Enge, P. "Global Positioning System, Vols I and II, Theory and Applications" American Institute of Aeronautics: Reston, VA, USA, 1996.
- [2] Hofmann-Wellenhof B, Lichtenegger H, Wasle E (2008) GNSS – GlobalNavigation Satellite Systems. Springer, Vienna, Austria
- [3] Teunissen PJ, Montenbruck O (2017) "Springer Handbook of Global Navigation Satellite Systems" Springer Cham, Berlin
- [4] Sanz J, Juan JM, Hernández-Pajares M, (2013) "GNSS Data Processing, Vol. I: Fundamentals and Algorithms; ESTEC TM-23/1" European Space Agency Communications: Noordwijk, The Netherlands.
- [5] <https://www.navcen.uscg.gov/?Do=constellationStatus>
- [6] <https://www.gsc-europa.eu/system-service-status/constellation-information>
- [7] <https://www.glonass-iac.ru/en/sostavOG/>
- [8] <http://en.beidou.gov.cn/>
- [9] European Union Agency for the Space Programme (2022) "EO and GNSS Market Report Issue 1, 2022". Publications Office of the European Union
- [10] International Telecommunication Union (2021) "ITU-R: Managing the radio-frequency spectrum for the world"
- [11] Kalman RE (1960) A New Approach to Linear Filtering and Prediction Problems. Transactions of the ASME–Journal of Basic Engineering 82, 35-45.
- [12] Ibáñez-Segura, D. Rovira-García A, Alonso, MT, Sanz J, Juan JM, González-Casado G, López-Martínez M. "EGNOS 1046 Maritime Service Assessment". Sensors 20.
- [13] Sanz J, Rovira-García A, Hernández-Pajares M, Juan JM, Ventura-Traveset J, López-Echazarreta C, "The ESA/UPC GNSS-Lab Tool (gLAB): An advanced educational and professional package for GNSS data processing and analysis", Proceedings of Toulouse Space Show 2012 4th International Conference on Space Applications, Jul. 2012
- [14] United States Department of Defense (2020).Global Positioning System Standard Positioning Service Performance Standard.
- [15] Beutler G, Rothacher M, Schaer S, Springer T, Kouba J, Neilan R. The International GPS Service (IGS): An interdisciplinary service in support of Earth sciences. Adv. Space Res. 1999, 23, 631–653 .
- [16] Montenbruck O, Steigenberger P, Prange L, Deng Z, Zhao Q, Perosanz FJ, Romero I, Noll CE, Stürze A, Weber G, et al (2017) "The Multi-GNSS Experiment (MGEX) of the International GNSS Service (IGS)–Achievements, prospects and challenges". Advances in Space Research 59, 1671–1697
- [17] International GNSS Service (2022) <https://igs.org/network/>
- [18] Klobuchar JA (1987). Ionospheric Time-Delay Algorithm for Single-Frequency GPS Users. IEEE Transactions on Aerospace and Electronic Systems 23, 325–331

The paper was originally published in the proceedings of 4rth Symposium on Space Educational Activities, Barcelona, April 2022 under a Creative Commons license : Attribution-NonCommercial-NoDerivs 4.0 International.

Copyright: Authors 2022.

The paper is republished here with permission. 

Determination of a GNSS-based velocity field of the African continent

This study provides for the entire continent of Africa the position/velocity solution precisely expressed with reference frame IGS03

Saturday E Usifoh

GFZ German Research Centre for
Geosciences, Potsdam, Germany
Institut für Geodäsie und
Geoinformationstechnik Technische
Universität, Berlin, Germany
Centre for Geodesy and Geodynamics,
Toro, Bauchi State, Nigeria

Benjamin Männel

GFZ German Research Centre for
Geosciences, Potsdam, Germany

Pierre Sakic

GFZ German Research Centre for
Geosciences, Potsdam, Germany

Joseph D Dodo

Centre for Geodesy and Geodynamics,
Toro, Bauchi State, Nigeria

Harald Schuh

GFZ German Research Centre for
Geosciences, Potsdam, Germany
Institut für Geodäsie und
Geoinformationstechnik Technische
Universität, Berlin, Germany

Abstract

GNSS-based velocity fields are a key tool to assess the boundaries around major deforming areas, to explain the main patterns of surface motion and deformation, to analytically review existing kinematics models and finally, to study the underlying tectonic activities. Determination of a velocity field for Africa is of great importance in the determination of the African Reference Frame; this is essential for better understanding the African plate tectonics. Therefore, this study focusses on the determination of the African velocity fields using continuously operated GNSS stations. We processed and analyzed 11 years of data obtained from a total number of 145 GNSS sites using GFZ's EPOS.P8 software. The result shows that Africa moves in the North-East direction. The station coordinates derived with PPP show averaged RMS values of 2.9 mm, 9.9 mm and 8.5 mm for the north, east and up components with respect to the estimated trajectory models. Horizontal velocities at sites located on stable Nubia plate fit a single plate model with residual motion below 1 mm/year of RMS. We confirm significant southeast motion in Morocco and Zambia with residual velocities of 1.4 mm/year and 0.9 mm/year, respectively. We estimate the Euler Poles for Nubia and Somalia with 48.59°N , -78.64°E , $0.264^{\circ}/\text{Myr}$ and 60.38°N , -83.33°E , $0.272^{\circ}/\text{Myr}$, respectively. Vertical velocities range from -2 to $+2$ mm/year, close to their uncertainties, with no distinct geographic pattern. The study also provides continental-wide

position and velocity field solution for Africa, and can also be considered as a contribution to the upcoming AFREF, the African Geodetic Reference Frame.

Introduction

The African Continent comprises of several cratons, stable blocks of old crust with deep roots in the subcontinental lithospheric mantle, and less stable terranes, which converged together to form the African Plate during the assembly of the supercontinent Pangea about 250 million years ago (Begg et al. 2009). The cratons include the Kalahari Craton, Congo Craton, Tanzania Craton, and West African Craton (see Fig. 1). The cratons were widely separated in the past, but brought together during the Pan-African orogeny and stayed together when Gondwana split up. The cratons are joined by orogeny belts, regions of highly deformed rock where the tectonic plates have engaged (Saria et al. 2013). The African plate that moved relatively slowly for the last 150 Ma (Lithgow-Bertelloni and Silveri 1998; Torsvik et al. 2010) is an interesting plate for studying intraplate magmatism. It contains various intraplate volcanic segments that are remote from the African plate boundaries. Such segment is the NE-SW oriented Cameroon Volcanic Line which bisects the angle where the coast of Africa makes a 90° bend from the western coast along the south of the West African craton and the southern coast along west of the Congo craton (see Fig. 1). It is characterized by

moderate magnitude earthquakes and active volcanism (Aka et al. 2004; Milelli et al. 2012). Moreso, the East African

Rift System (EARS), is a place where the Earth's tectonic forces create new plates by splitting apart old ones. In other words,

it is a fracture in the Earth's surface that widens over time. The Nubian Plate makes up most of Africa, while the smaller plate that is pulling away is named Somalian Plate. These two plates are moving away from each other and also away from the Arabian plate to the north (Chu and Gordon 1999). The point where these three plates meet is the triple-junction at the Afar region of Ethiopia. However, all the rifting in East Africa is not confined to the Horn of Africa; it further extends to south into Kenya, Tanzania and Great Lakes region of Africa. The East African Rift system reaching from the Afar in the northern Ethiopia to Mozambique in the south shows spreading rates of up to 5 mm/year (Saria et al. 2013).

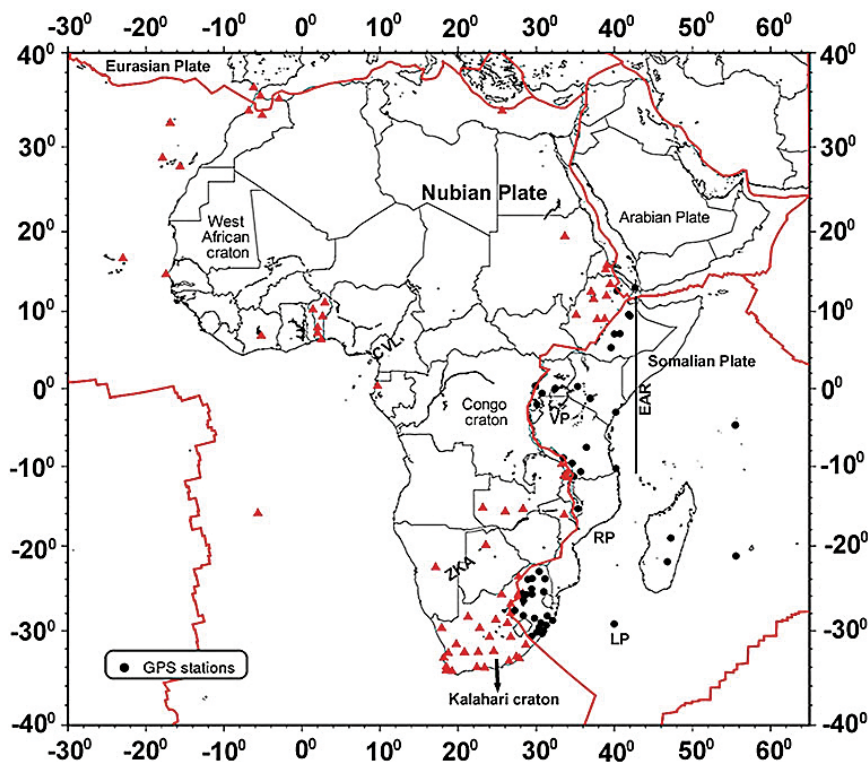


Fig. 1 Map showing the major tectonic setting of Africa, the Craton and the GNSS stations used in this study. VP Victoria Plate, LP Lwandle Plate, RP Rovuma Plate, ZKA Zimbabwe-Kalahari Axis, CVL Cameroon Volcanic Line. Red triangle (GPS stations used to compute Euler vector in Nubian Plate), black dots (GPS stations used to compute Euler vector in Somalian Plate), and solid red line shows the major plate boundaries as given in the PB2002 model (Bird et al. 2002)

The dynamics of the tectonic plate activities of the Earth are the major causes for ground motion. Beginning from the mid-1980s, the Global Navigation Satellite Systems (GNSS) have been effectively used in determining plate tectonic movement and other geodynamic phenomena. Over the last years, the monitoring of station coordinates located on the Earth's surface has become a great interest. Determination of velocity fields produces the means of analysing intra- and inter-plate geodynamic interactivities and other crustal disturbances (Holden et al. 2017; Kierulf et al. 2021). Saria et al. (2013) carried out some geodynamic studies for Africa from the combined GPS and DORIS space geodetic solutions, and observed that the velocity on the stable Nubia fits to a single rigid plate model with a WRMS of 0.6 mm/year, that is consistent with the current uncertainty of geodetic measurements in the region. Investigation of GNSS-based monitoring of continental-wide variations in Africa (Nubia) and Arabia plate shows that there is little variation in rates of motion along the boundary, ranging from 5.4 ± 1 mm/year in the eastern Mediterranean to 4.5 ± 1 mm/year near Gibraltar (McClusky et al. 2003), hence, this study tends to focus on the determination of velocity field for Africa.

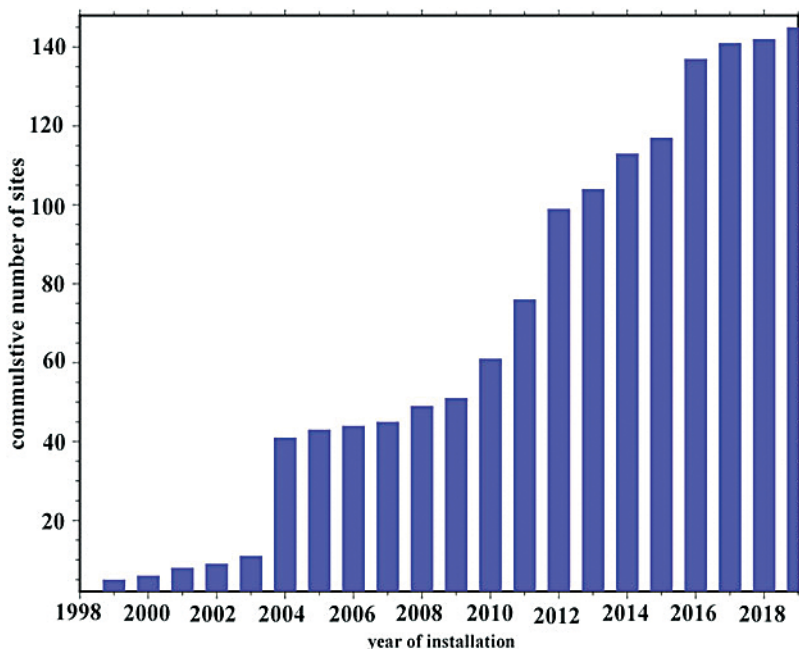


Fig. 2 Bar chart showing the cumulative number of continuous GNSS stations in Africa from 1998 to 2019. There was a speedy increase from 2004 to 2019

This introduction is followed by Sect. 2 the methodology and processing strategies. Section 3 presents the results, and Sect. 4 conclusions and recommendations.

Input Data

GNSS Data Collection and Processing

The GNSS data set used in this study includes 11 years of observations (2009–2019) from GNSS sites where data are openly available (see Fig. 1). A total number of 145 GNSS sites were used and the data were obtained from TrigNet¹ a network of continuously operating system base stations that are located in South Africa, from the UNAVCO archive² and the AFREF archive.³ There are other GNSS network stations in Africa that are operating but unfortunately, could not be included due to data restriction. All openly available GNSS data used in this paper were processed; stations less than 3 years of observations were skipped. This is slightly above 2.5 years which is the minimum amount of time required to average out seasonal signals unrelated to the long term motions of interest in order to obtain a good velocity estimate (Blewitt and Lavallée 2002). There has been a rapid increase of GNSS stations in the years from 2004 to 2019 (see Fig. 2).

We analyse the GNSS data in PPP mode using the GFZ's EPOS.P8 software, based on GFZ repro3 solution (Männel et al. 2020). Precise point positioning (PPP) method is a robust method that focused on the processing of measurements from stand-alone GNSS receivers to compute high accurate positions (Zumberge et al. 1997), and has become cost effective in achieving centimeter-level accuracy. GNSS orbit modelling, satellite clocks and Earth Rotation Parameters (ERP) from GFZ repro3 were introduced apriori (Männel et al. 2021). We processed zero-differenced GPS observations using ionosphere-free linear combination with a 5 min sampling rate, to estimate daily station coordinates and tropospheric delays with 1 h ZTD and 24 h troposphere gradients.

Phase ambiguities were not re-solved but estimated. We applied models following the IERS 2010 Conventions (Petit and Luzum 2010) and repro3 setup.⁴ As the orbit products are provided in the repro3-specific reference frame, our coordinates are determined in this IGS03 frame (Rebischung 2021). To ensure consistency, GNSS phase center corrections given in `igsR3_2077.atx` were applied.

These daily solutions were used to generate position time series, which we closely inspected to identify outliers, offsets, or discontinuities. Coordinate and data conversion were done based on the GeodeZYX toolbox (Sakic et al. 2019). Subsequently, we used the Sari software (Santamaría-Góm 2019), to model site positions as the sum of (1) linear term representing secular displacement (2) offsets caused by earthquakes, and other effects, mostly equipment changes and (3) periodic components. The model equation for each of the component (east, north, up) is given below

$$y = a + bt + \sum_{i=1}^N ciGi(t) + d \sin(2\pi t) + e \cos(2\pi t) \quad (1)$$

where a is the coordinate (initial position at reference epoch), b is the linear velocity (trend), c are the discontinuities, d and e are the annual amplitudes, t is the time epoch, G_i is the binary operator equal to zero, if t is less than zero or equal to 1, if t is greater or equal to zero, respectively. Sites, especially those with frequent offsets, including, PRE1, PRE2, HRAO (all in South Africa), NAZR, DAFT (all in Ethiopia) showed too many outliers and offsets and were therefore excluded from the final solution.

Results and discussion

Raw Time Series, FUNC (Madeira Island, Portugal) and LSMH (Ladysmith, South African)

From the raw coordinate time series, in the north and east components of the two stations, a linear trend is observed with a pronounced positive slope which shows north-east motion of 27 ± 0.3 mm/

year. Moreover, it can be observed that the height (up) component is quite noisier than the horizontal components which are due to observation geometry. In order to model the station trajectories, we used Eq. (1) to estimate the linear trend, annual signals and discontinuities. The estimated linear trend and the residual coordinates are shown in Fig. 3 and Table 1.

As shown in Fig. 3, FUNC and LSMH move with 17–18 mm/year towards north. The east component shows a similar trend for both stations with a velocity of 15–17 mm/year. We compared the velocity results computed using PPP solutions with the velocity results computed using UNAVCO plate motion calculator with respect to GSRM2.1 (Kreemer et al. 2014) (see Table 2), though there is a difference of 1.0–1.6 mm/year and 0.9–1.3 mm/year in the north and east direction, respectively, their difference is insignificant. For the vertical component their velocities are 0.6 ± 0.2 mm/year and 0.4 ± 0.2 mm/year, respectively. This slight motion could be from vertical uplift movements caused by atmospheric pressure variation and mass loading redistribution of non-tidal ocean loading and soil moisture (El-Fiky et al. 1997). The up component shows yearly variations with deterministic model (shown in red) containing harmonics, based on the least-squares approach. We notice in the up components, periodic surface deformations of about 25 mm, which are not apparent in the north and east components. These surface deformations are believed to be due to a large influence of non-tidal loading especially hydrological loading (Männel et al. 2019; Liu et al. 2017). We compared our velocity estimates against the ITRF2014 and found only minor discrepancies of 1–0 mm/year and 0 to –0.1 mm/year in the North and the East direction, respectively.

Figure 4 shows detrended data of the two selected stations FUNC and LSMH. The Root Mean Squares (RMS) of the residuals, i.e. the observed minus the computed, are 4.4 mm, 8.1 mm, 8.6 mm and 2.2 mm, 6.7 mm, 7.4 mm for the north, east and up components,

respectively. We observe in Table 1 that the RMS in the north component is smaller than that of the east components in both stations, and highest in the up components. This is related to (1) observation geometry and (2) that the ambiguities are not fixed (float solution), which is causing a larger

RMS in the east component. In addition, considering both stations, we observed that the RMS of station FUNC is higher in all the components than that of station LSMH, which shows that station LSMH is more stable to that of the station FUNC. This is most probably related to the station

monuments as FUNC is located at the terrace of an old building whereas station LSMH is located on a concrete block.

Figure 5 shows the horizontal velocity fields for the whole Africa. We grouped the horizontal and vertical velocity field

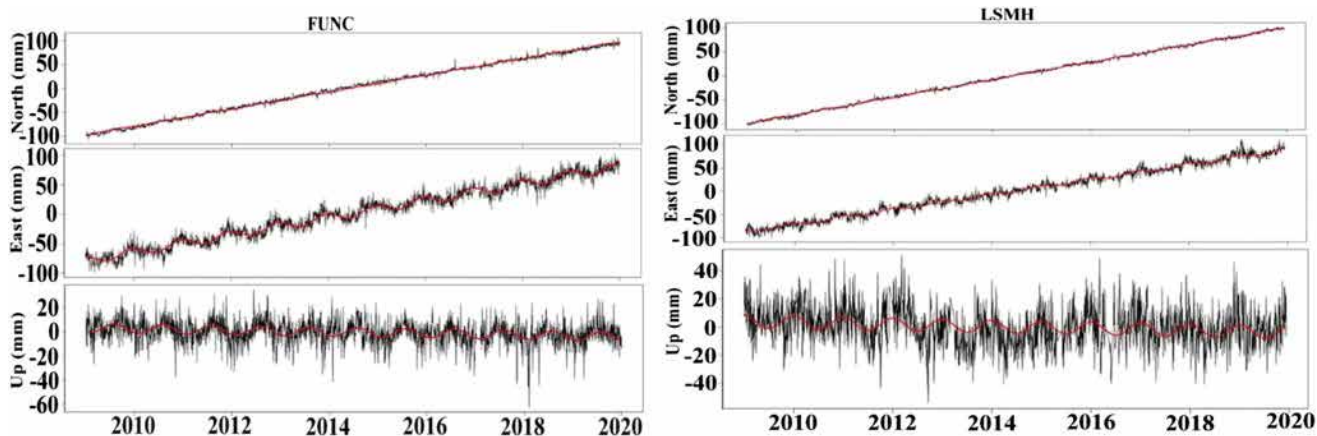


Fig. 3 Time series of the GNSS stations FUNC (Madeira Island, Portugal) and LSMH (Ladysmith, South African) using combined function of linear and sinusoidal approach

Table 1 Time series characteristics (velocities, root mean squares, and annual amplitudes for north, east and up components) for stations FUNC and LSMH

Station	Velocities (mm/year)			RMS (mm)			Annual ampl. (mm)		
	North	East	Up	North	East	Up	North	East	Up
FUNC	17 ± 0.1	15 ± 0.1	0.6 ± 0.2	3.4	8.1	8.6	0.9 ± 0.1	7.1 ± 0.2	3.7 ± 0.2
LSMH	18 ± 0.0	17 ± 0.1	0.4 ± 0.2	2.2	6.7	7.4	1.2 ± 0.2	3.5 ± 0.1	2.5 ± 0.2

Table 2 Comparison of horizontal velocities computed with UNAVCO plate motion calculator

Station	Velocities (mm/year) computed with model GSRM2.1 (2014)		Velocities (mm/year), GNSS (this study)		Difference (mm/year)	
	North	East	North	East	North	East
FUNC	18.0	15.1	17.0	15.0	1.0	0.1
LSMH	19.6	18.3	18.0	17.0	1.6	1.3

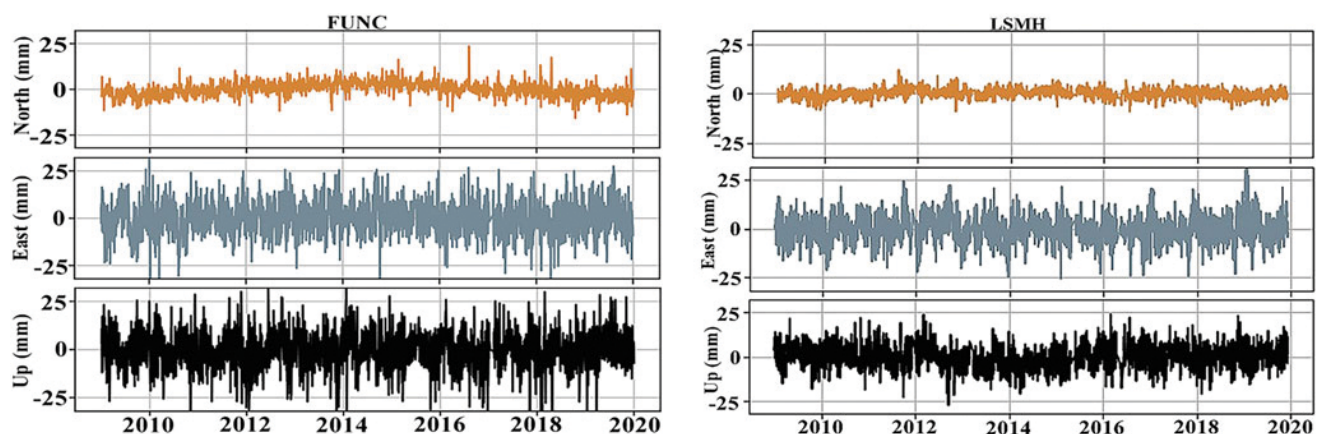


Fig. 4 Detrended linear characteristics in time series of the GNSS stations FUNC (Madeira Island, Portugal) and LSMH (Ladysmith, South African)

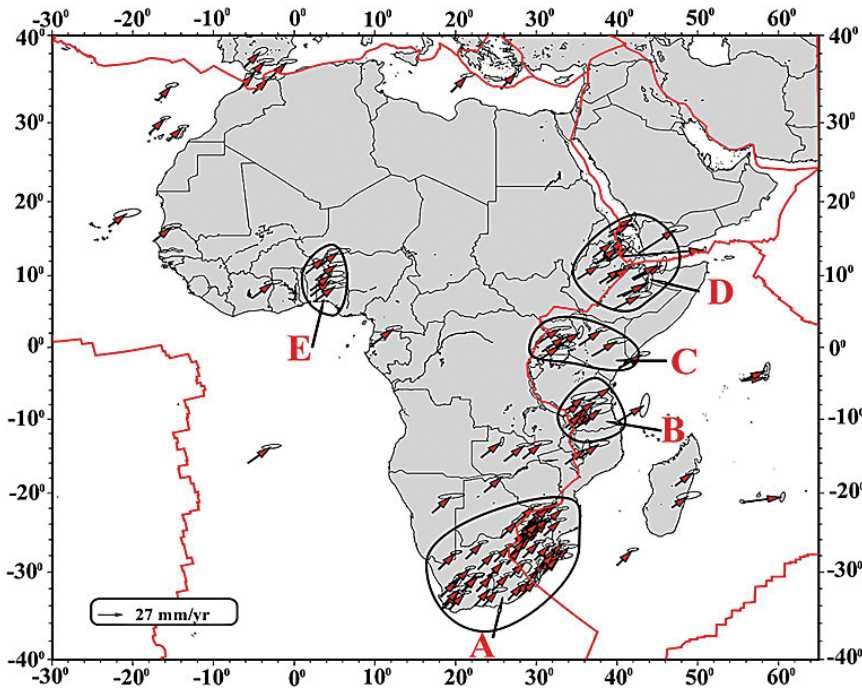


Fig. 5 Horizontal velocity with respect to IGSR3 and error ellipses of 95% confidence level

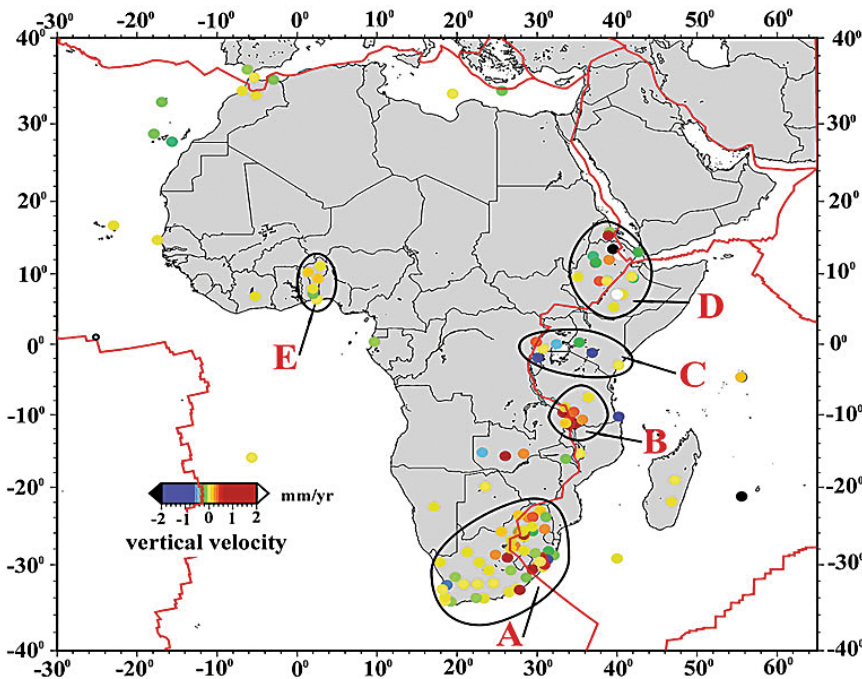


Fig. 6 Vertical velocities with respect to IGSR3 derived from this study

estimates into different groups A, B, C, D and E as indicated in Figs. 5 and 6, according to their velocity pattern. From our observations, the estimated horizontal geodetic velocities show completely the same pattern, thus indicating that African plate moves as rigid plate in north east direction with respect to the IGSR3 reference frame with velocity field of each group and their corresponding root mean square given Table 3.

The mean horizontal velocity for the overall block in north east direction is 27 ± 0.3 mm/year with average root mean square residuals for north, east and up components of 2.9 mm, 9.9 mm and 8.5 mm respectively. Looking at B (Tanzania) and E (Benin Republic), we observe that their horizontal velocities are the same which shows that the two blocks are moving in north east direction at the same rate. In addition, for group C (Kenya, Rwanda and Uganda) and group D (Ethiopia), their velocities stand out with a slight local velocity difference with respect to IGSR3 due to their location on the great valley rift (stratovolcano), as previous studies have shown that the African continent is undergoing continuous rifting along the East African Rift System (Ring 2014; Gaina et al. 2013). Considering group A (South Africa), stations KOKS (Kokstad), DRBN (Durban), STAN (Stanger) and GREY (Greytown), located in the Kwa-Zulu Natal province exhibit different but significant vertical displacement of velocity values of $+1.5 \pm 0.2$ mm/year, $+1.7 \pm 0.3$ mm/year, $+1.8 \pm 0.3$ mm/year and $+1.6 \pm 0.3$ mm/year, respectively. Stations KOKS, DRBN and STAN all in Kwa-Zulu Natal show uplift, which could be due to seismically active zones (one lesser, one greater in linear extent) across the continent ocean boundary at high angle (Hartnady 1990). In group

Table 3 Horizontal and vertical velocity and the root mean square of each group according to their patterns

	Group A (South Africa)	Group B (Tanzania)	Group C (Kenya/Rwanda/Uganda)	Group D (Ethiopia)	Group E (Benin Rep.)
Horizontal velo. (mm/year)	25 ± 0.1	29 ± 0.1	31 ± 0.1	32 ± 0.2	29 ± 0.1
Vertical velo. (mm/year)	1.3 ± 0.1	1.9 ± 0.2	1.5 ± 0.2	5.2 ± 0.2	0.4 ± 0.2
RMS (mm)	4.9	5.8	5.3	5.9	7.2
Ampl. (mm)	2.6 ± 0.2	2.4 ± 0.3	2.1 ± 0.2	2.8 ± 0.5	3.2 ± 0.5

B (Tanzania), we observed a significant change which probably indicates an uplift vertical displacement of velocity field approximately ranging from -2 to $+2$ mm/year; in agreement with Saria et al. (2013). As anticipated, uncertainties expeditiously decrease with time series length.

Euler Pole parameter estimation

We generated a rigid plate model by estimating plate rotations (Euler poles). Hence, we group the stations according to their location (Fig. 5), while testing the rigid plate assumption. We estimate the rotation rate vector for the Nubian and the

Somalian plate and tested the significance relative to the IGSR3 interpretation using sites outside the deformation zones along the plate boundaries, and by excluding nearby redundant sites (Fig. 7). Stations NAZR, DABT and HERM were removed after outlier detection. Previous reports of Nubian and Somalian plate uses fewer sites, so we define a new subset of sites with a larger and better geographic distribution (Saria et al. 2013). The angular velocity of the Nubian plate with respect to IGSR3 (Table 4 and Fig. 7) is close to the recent estimate of Altamimi et al. (2017). The uncertainty associated with this new angular rotation of Nubia with respect to

IGSR3 so far is the smallest, most likely because the solution presented in this study is based on a larger number of GNSS sites and longer observation time span.

Nevertheless, a significant limitation is the lack of dense, homogeneous continuous GNSS network over most of the Africa. With respect to stable part of Nubia, the residual velocities as given in Fig. 7, shows regions with significant deformation. It is expected that in the eastern part of the East African Rift, larger residuals are observed as this region contains various microplates (Wedmore et al. 2021). We also observed a deviation from the plate rigidity in stations RABT, IFRI, TETN in Morocco and MONG in Zambia with their residual velocities tended towards SSE at average velocities 1.4 mm/year and 0.9 mm/year respectively.

For the Somalian plate, we selected 55 GNSS stations to estimate site velocities as shown in (Fig. 1). We observed that stations in the volcanically active island Reunion (Fig. 7) have velocities that are agreeing with the rigid Somalian and could therefore be used to define its kinematics. Stations NEGE and ROBE (Ethiopia), located 15 km from the rift, and MTDK (Tanzania), located 100 km from the Tanzania Rift, are also agreeing with rigid Somalian.

Conclusions

In this study, we processed data of 145 stations from 2009 to 2019 with GFZ EPOS.P8 solution in PPP mode. These data sets were taken from a geodetic network precisely designed and surveyed to measure tectonic motion through the South African network, UNAVCO and

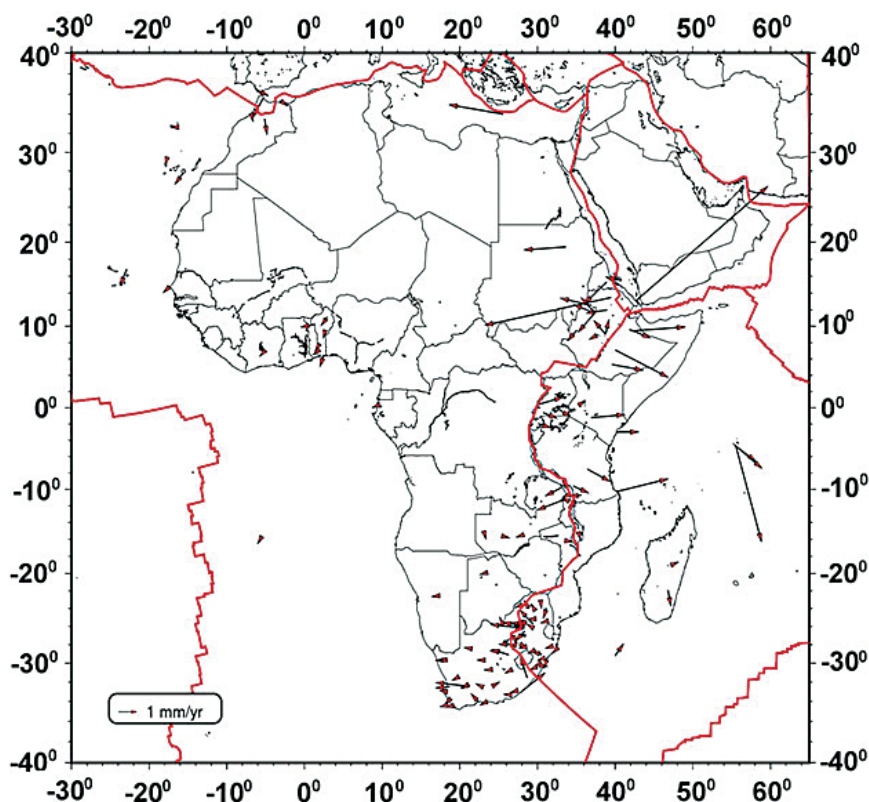


Fig. 7 Residuals of the observed plate-fixed velocities relative to the modelled using the estimated Euler Pole with respect to Nubia and Somalian plate

Table 4 Estimated plate kinematic parameters

Plate (IGSR3)	Num. of sites	Lat (deg)	Long (deg)	ω_x (mas/year)	ω_y (mas/year)	ω_z (mas/year)	Angular velocity ($^{\circ}$ /Myr)	WRMS	
								E (mm/year)	N (mm/year)
Nubian \pm	79	48.59	-78.64	0.035	-0.174	0.201	0.264 ± 0.000	0.12	0.17
		0.265	0.611	0.002	0.000	0.001			
Somalian \pm	55	60.38	-83.33	0.016	-0.134	0.237	0.272 ± 0.017	0.21	0.17
		0.238	0.407	0.009	0.006	0.020			
ITRF2014				Altamimi et al. (2017)					
Nubian \pm	24	48.79	-80.33	0.099	-0.614	0.733	0.267 ± 0.001	0.28	0.36
		0.290	0.110	0.004	0.003	0.001			
Somalian \pm	3	49.24	-94.15	-0.121	-0.794	0.332	0.332 ± 0.882	0.32	0.30
		0.260	0.720	0.035	0.034	0.008			

This study provides for the entire continent of Africa the position/velocity solution precisely expressed with reference frame IGSR3

AFREF. The resulting coordinates were used to determine the horizontal and vertical velocity fields with respect to IGSR3. The linear trends in the coordinate time series were estimated by fitting a trend to the data and estimate its velocity coefficients using the least-squares principle. We observed that Africa is moving in north-east motion with respect to IGSR3 with the overall horizontal average velocity field of 27 ± 0.3 mm/year and with vertical uplift in Tanzania with velocity field ranging from -2 to $+2$ mm/year; other regions show no significant changes. Moreover, the present availability of geodetic sites in Africa is not even and the intra-plate deformation at regional or local scales with the current networks may not be detectable.

This study provides for the entire continent of Africa the position/velocity solution precisely expressed with reference frame IGSR3, and hence it will serve as a base in the contribution to the computation of the velocity field of Africa in the determination of the upcoming African Reference Frame AFREF and also gives a better understanding of the African plate tectonics, that appears to be lacking in earlier studies of the AFREF reports. Though much effort has been made on GNSS site distribution in Africa, most part of the African continent still remains undersampled. Effort to augment the geodetic infrastructure is under way, through link academic research projects, AFREF or in the level of surveying applications. Hence, the objective of this new data will help in the establishment and maintenance of a unified geodetic reference network for Africa which will serve as a fundamental basis for national reference networks that will fully be consistent and homogeneous with the global reference frame of the International Reference Frame (ITRF).

Acknowledgements

The authors would like to thank and express their gratitude to the South African Network (TrigNet), UNAVCO, AFREF, and IGS (Johnson et al. 2017) for making their GNSS data available.

Availability of data and materials

The data used to support the findings of this study are available on their website cited as footnote.

Conflict of interest The authors declare that they have no conflicts of interest.

Authors' contributions Saturday Ehisemhen Usifoh downloaded the data, processed, analysed and wrote the manuscript. BM, PS, DJ, and HS verified the feasibility of the method, checked the processing, the analysis, the interpretation, and the discussion of the results. All authors joined in revising the manuscript and figures modification.

Code availability Not applicable.

Ethics approval and consent to participate Not applicable.

Consent for publication Not applicable.

Funding Not applicable.

End notes

¹ <http://data.unavco.org/archive/gnss/rinex/obs/>: Date access 9th June, 2020.

² <http://afredata.org/>: Date access 25th August, 2020.

³ <ftp://ftp.trigent.co.za/>: Date access 13th September, 2020.

⁴ <acc.igs.org/repro3/repro3.html>: Date access: 15th January, 2021.

References

- Aka FT, Keisuke N, Minoru K, Hirochika S, Greg T, Bekoa A, Joseph H (2004) Symmetrical Helium isotope distribution on the Cameroon Volcanic Lines, West Africa. *Chem Geol* 203(3–4):205–223. <https://doi.org/10.1016/j.chemgeo.2003.10.003>
- Altamimi Z, Métivier L, Rebischung P, Rouby H, Collilieux X (2017) ITRF2014 plate motion model. *Geophys J Int* 209:1906–1912. <https://doi.org/10.1093/gji/ggx136>
- Begg GC, Griffin WL, Napapov LM, O'Reilly SY, Grand SP, O'Neill CJ, Hronsky JMA, Poudjom Djomani Y, Swan CJ, Deen T, Bowden P (2009) The lithospheric architecture of Africa: seismic tomography, mantle petrology and tectonic evolution. *Geosphere* 5:23–50. <https://doi.org/10.1130/GES00179.1>
- Bird P, Kagan YY, Jackson DD (2002) Plate tectonics and earthquake potential of spreading ridges and oceanic transform faults. In: Stein S, Freymueller JT (eds) *Plate boundary zones, Geophysical monograph series, vol 30*. AGU, Washington DC, pp 203–218. <https://doi.org/10.1029/GD030p0203>
- Blewitt G, Lavallée D (2002) Effect of annual signals on geodetic velocity. *J Geophys Res* 107(B7):2145. <https://doi.org/10.1029/2001JB000570>
- Chu D, Gordon RG (1999) Evidence for motion between Nubia and Somalian along the southwest Indian. *Nature* 398:64–67. <https://doi.org/10.1038/18014>
- El-Fiky GS, Teruyuki K, Yoichiro F (1997) Distribution of vertical crustal movement rates in the Tohoku district, Japan, predicted by least squares collocation. *J Geod* 71:432–442. <https://doi.org/10.1007/s001900050111>
- Gaina C, Torsvik TH, van Hinsbergen DJJ, Medvedev S, Werner SC, Labails C (2013) The African plate:

- a history of oceanic crust accretion and subduction since the Jurassic. *Tectonophysics* 604:4–25. <https://doi.org/10.1016/j.tecto.2013.05.037>
- Hartnady CJH (1990) Seismicity and plate boundary evolution in southeastern Africa. *S Afr J Geol* 93(3):473–484. https://hdl.handle.net/10520/AJA10120750_853
- Holden L, Silcock D, Choy S, Cas R, Ailleres L, Fourmiers N (2017) Evaluating a campaign GNSS velocity field derived from an online precise point positioning service. *Geophys J Int* 208:246–256. <https://doi.org/10.1093/gji/ggw372>
- Johnson G, Riddell A, Housler G (2017) *The International GNSS service*. Springer, Cham, pp 967–982. <https://doi.org/10.1007/978-3-319-42928-1>
- Kierulf HP, Steffen H, Barletta VR, Lidberg M, Johansson J, Kristiansen O, Tarasov L (2021) A GNSS velocity field for geophysical applications in Fennoscandia. *J Geodyn* 146:101845. <https://doi.org/10.1016/j.jog.2021.10184>
- Kreemer C, Blewitt G, Klein EC (2014) A geodetic plate motion and Global Stain Rate Model. *Geochem Geophys Geosyst* 15:3849–3889. <https://doi.org/10.1002/2014GC005407>
- Lithgow-Bertelloni C, Silveri PG (1998) Dynamics topography, plate driving forces and the Africa superwell. *Nature* 395:269–272. <https://doi.org/10.1038/26212>
- Liu L, Khan SA, van Dam T, Ma JHY, Bevis M (2017) Annual variations in GPS-measured vertical displacements near Upernavik Isstrøm (Greenland) and contributions from surface mass loading. *J Geophys Res Solid Earth* 122:677–691. <https://doi.org/10.1002/2016JB013494>
- Männel B, Dobsław H, Dill R, Glaser S, Balidakis K, Thomas M, Schuh H (2019) Correcting surface loading at the observation level: impact on global GNSS and VLBI station networks. *J Geod* 93:2003–2017. <https://doi.org/10.1007/s00190-019-01298>
- Männel B, Brandt A, Bradke M, Sakic P, Brack A, Nischan T (2020) Status of IGS reprocessing activities at GFZ. In: *International Association of Geodesy Symposia*. Springer, Heidelberg. https://doi.org/10.1007/1345_2020_98
- Männel B, Brandt A, Bradke M, Sakic P, Brack A, Nischan T (2021) GFZ repro3 product series for the international GNSS service (IGS). GFZ Data Services. <https://doi.org/10.5880/GFZ.1.1.2021.001>
- McClusky S, Reilinger R, Mahmoud S, Ben D, Tealeb A (2003) GPS constraints on Africa (Nubia) and Arabian plate motions. *Geophys J Int* 155:126–138. <https://doi.org/10.1046/j.1365-246X.2003.02023>
- Milelli L, Fourel L, Jaupart C (2012) Lithospheric instability origin for the Cameroon Volcanic Line. *Earth Planet Sci Lett* 335–336:80–87. <https://doi.org/10.1016/j.epsl.2012.04.028>
- Petit G, Luzum B (2010) *IERS conventions*. IERS technical note 36. Verlag des Bundesamts für Kartographie und Geodäsie, Frankfurt am Main. ISBN: 3–89888–989-6
- Rebischung P (2021) IGS3_2077.atx. <https://doi.org/10.5190/egusphere-egu21-2144>
- Ring U (2014) The East African rift system. *Aust J Earth Sci* 107:132–146
- Sakic P, Ballu V, Mansur G (2019) The GeodeZYX toolbox: a versatile python 3 toolbox for geodetic-oriented purposes. V. 4.0 GFZ Data services. <https://doi.org/10.5880/GFZ.1.1.2019.002>
- Santamaría-Góm A (2019) Sari: interactive GNSS position time series analysis, vol (0123456789). Part of Springer Nature (2019, online). <https://doi.org/10.1007/s10291-0846-y>
- Saria E, Calais E, Altamimi Z, Willis P, Farak H (2013) A new velocity field for Africa from combined GPS and DORIS space geodetic solutions: contribution to the definition of the African reference frame (AFREF). *J Geophys Res Solid Earth* 118:1677–1697. <https://doi.org/10.1002/jgrb.50137>
- Torsvik TH, Steinberger B, Gurnis M, Gaina C (2010) Plate tectonic and net lithosphere rotation over the past 150 My. *Earth Planet Sci Lett* 291:106–112. <https://doi.org/10.1016/j.epsl.2009.12.055>
- Wedmore LNJ, Biggs J, Floyd M, Fagereng Å, Mdala H, Chindandali P et al (2021) Geodetic constraints on cratonic microplates and broad strain during rifting of thick Southern African lithosphere. *Geophys Res Lett* 48:e2021GL093785. <https://doi.org/10.1029/2021GL093785>
- Zumberge JF, Heflin MB, Jefferson DC, Watkins MM, Webb FH (1997) Precise point positioning for the efficient and robust analysis of GPS data from large networks. *J Geophys Res* 102(B3):5005–5017. <https://doi.org/10.1029/96JB03860>

Open Access This chapter is licensed under the terms of the Creative Commons Attribution 4.0 International License (<http://creativecommons.org/licenses/by/4.0/>), which permits use, sharing, adaptation, distribution and reproduction in any medium or format, as long as you give appropriate credit to the original author(s) and the source, provide a link to the Creative Commons license and indicate if changes were made.

The images or other third party material in this chapter are included in the chapter's Creative Commons license, unless indicated otherwise in a credit line to the material. If material is not included in the chapter's Creative Commons license and your intended use is not permitted by statutory regulation or exceeds the permitted use, you will need to obtain permission directly from the copyright holder.

The paper was first published in International Association of Geodesy Symposia. The paper is republished with authors' permission.

© The Author(s) 2022 

MAGICA project: Crossed IFA Multi-frequency GNSS Integrated Cost-effective Antenna for Automotive Applications

The present paper shows the prototype results of the antenna designed in the scope of the MAGICA project providing a multi-constellation and multi-band (L1/E1, L5/E5 and E6) solution for the automotive industry

Marco Antonio Vélez

IDNEO Technologies,
S.A.U, Carrer Rec de Dalt,
3, 08100 Mollet del Vallès
(Barcelona), Spain

Jose Javier Vicente

IDNEO Technologies,
S.A.U, Carrer Rec de Dalt,
3, 08100 Mollet del Vallès
(Barcelona), Spain

Joan Gemio

IDNEO Technologies,
S.A.U, Carrer Rec de Dalt,
3, 08100 Mollet del Vallès
(Barcelona), Spain

Laia Vilalta

IDNEO Technologies,
S.A.U, Carrer Rec de Dalt,
3, 08100 Mollet del Vallès
(Barcelona), Spain

Laura Tantinyà

IDNEO Technologies,
S.A.U, Carrer Rec de Dalt,
3, 08100 Mollet del Vallès
(Barcelona), Spain

Alberto Gil

SEAT S.A., Autovia A-2,
km 585, 08760 Martorell
(Barcelona), Spain

Adrián Cardalda

Rohde & Schwarz GmbH &
Co. KG, Muehldorfstrasse 15,
81671 Munich, Germany

Daniel Baños

IDNEO Technologies,
S.A.U, Carrer Rec de Dalt,
3, 08100 Mollet del Vallès
(Barcelona), Spain

Pere Mogas

IDNEO Technologies,
S.A.U, Carrer Rec de Dalt,
3, 08100 Mollet del Vallès
(Barcelona), Spain

Joaquín Reyes

EUSPA, European Union
Agency for the Space
Programme, Janovskeho
438/2, 17000 Prague 7,
Holesovice, Czech Republic

Abstract

The present work describes the project of a multi-band GNSS compact antenna for high precision positioning applications for the automotive industry (MAGICA project). The following results correspond to the final prototyping phase. The main objective of the project is to develop an innovative, compact, low-cost antenna for high accuracy positioning applications following the standards of the automotive market. The antenna operates in several frequency bands, including L1/E1, L5/E5 and E6, and can operate over different positioning satellite constellations like Galileo or GPS. The development of GNSS receivers for multiple band operation is consolidated in certain markets, but the challenges of the automotive market require a robust and high-performance antenna design in a compact solution at a competitive cost. The project is facing the final prototyping phase. There have been several design loops together with the mechanical department, to reach a feasible and cost-effective antenna system ready for mass-production, suitable for the autonomous driving operation. Before the definitive integration in vehicle, the prototype obtained provides really promising results in free space environment. The antenna, besides being technically and cost-competitive, fulfils the mechanical and electronic design requirements of the automotive sector.

Introduction

Fully autonomous vehicles are expected to be a reality by 2040, but vehicles with autonomous capabilities will be a reality much sooner (2024-2025) [1]. One of the main challenges for autonomous vehicles is to have a high accurate, instant available and robust positioning. The vehicle should know in every moment its absolute position and its relative position with reference to the rest of the vehicles, objects and people in the surrounding; this is one of the key aspects for autonomous driving safety [2].

Absolute positioning makes reference to the ability to locate the vehicle in a map. The receivers rely on the GNSS service to provide the absolute positioning [3]. With the revitalization of the GLONASS constellation and the emerging constellations Galileo and BeiDou together with the traditional one (GPS), the possibility to get an available, reliable and accurate positioning has increased [3].

The work presents the measured technical results of a first prototype of the cost-competitive antenna for the automotive market, providing a multi-band and multi-constellation solution. Current antennas in the automotive market are commonly dual frequency antennas covering a combination of L1 with one of these two other GNSS frequency bands, L2 or L5. The antenna presented can receive simultaneously at least L1/E1, L5/E5 and E6 bands fulfilling the defined requirements. The L5 band lowers the risk of interference, improves the multipath protection and it also makes easier the reception of the non-data signals (pilot signal, synchronization...) in unfavourable and obstructed conditions. This is the reason why it was preferred to cover L5 as a design requirement over the L2 band. The operation capability on the E6 band is one of the distinguishing features of the design, E6 provides a high data rate transmission making it ideal for applications that require global, high-accuracy positioning. At later stages of the project, it will be evaluated the influence of the vehicle structure on

the response of the antenna by means of vehicle level measurements of the antenna inside a real vehicle spoiler.

Multi-constellation and multi-frequency antennas can be found in other markets [4] [5], but they do not fit the specific constraints of the automotive sector: compact size, robustness, cost-competitive, and suitable for high dynamic receivers. The design should meet all those constraints while ensuring the needs of the safety for autonomous driving applications.

A common approach for the design of automotive GNSS antennas is to use ceramic patches with a narrow band response. This approach has been adequate for single band operation for being very compact, low-profile structures that can achieve a good performance at a low cost. However, to cover multiple bands with a higher bandwidth, this kind of solution is not optimal. In general, the approach of the antenna makers is the use of stacked patch structures to obtain this multi-frequency behaviour [6]. To achieve acceptable operating bandwidths, multiple and very large stacked patches are used making the weight and cost very high [7]. With lower patch bandwidths, the range of operation and/or the performance are not very suitable. In addition, a large ground plane would help maximize the performance of the GNSS patch antennas. However, the position of the antenna on the ground plane affects directly to an antenna particular tuning, with the direct impact on the integration in the vehicle.

In contrast, the MAGICA antenna is a solution based on a metal sheet volumetric topology, which allows the desired multi-frequency behaviour with a wide bandwidth, while remaining a low cost and a very low weight antenna. Being a standalone solution, the antenna does not need any additional ground plane for its optimal operation, improving the in-vehicle integrability.

One of the main challenges is to meet all the requirements while ensuring the manufacturability of the antenna, which has a major impact on the cost.

After the simulation stage (as presented in [8]), it is time to develop the prototypes that confirm the performance of the design. The results of this prototyping stage, the associated technical results of the measurements and the steps to follow will be explained through the paper.

IDNEO is involved in the development of the design and the coordination of the consortium of the MAGICA stakeholders. Additionally, the consortium is composed by the car manufacturer SEAT S.A. which provides the requirements in terms of cost and integration and a specific vehicle model to integrate the antenna under test, and Rohde & Schwarz that develops and provides all the RF and instrumentation equipment necessary to test the antenna capabilities, including the novel Galileo E6 band.

The paper presents a brief explanation of the methodology applied during the project in section 2. It is followed by the results of the technical performance in section 3 including the measurements of the radiating element or passive antenna, RF front-end amplifier and also the entire system (active antenna) at prototyping stage. Section 4 presents main conclusions and the future next steps.

Antenna requirements and design methodology

The results presented in this paper are the consequence of all the design loops (i.e., component research and definition, simulation, prototyping and validation), manufacturability studies, economic analysis, etc. with the relevant disciplines involved in the whole process such as RF, HW, mechanical engineering, purchasing department among others. The main design target when checking whether the antenna is aligned to the project might seem the RF technical requirements that provide high accuracy positioning. However, there is also a cost-effective goal very important in the automotive sector that is strongly related to the manufacturing process. This manufacturing process not only has to be feasible to keep a reasonable cost, but also has not to alter the technical

performance. Therefore, a trade-off among these three aspects is always present along the design phase of the project.

The design process has been performed in several steps.

The radiating element was designed with a 3D electromagnetic solver for antenna design and includes a polariser circuit; the RF front-end amplifier was developed by means of an electronic and electromagnetic solver for RF circuit design. Once a candidate design of the two electronic components was achieved, the prototype stage started, following the methodology aforementioned.

For its characterization, a multi-probe system in an anechoic chamber in free space condition has been used for near-field measurement of the radiation pattern measurement. The free space condition means that the antenna is in a condition

in which there are neither interfering signals (reflections), nor objects or materials that might alter the antenna's radiation properties. As it is shown in Figure 1, the MAGICA antenna has been characterized in free space condition (antenna alone) as well as with the antenna integrated in the spoiler environment.

At the later stages of the project, the antenna performance is going to be evaluated integrated inside a vehicle (provided by SEAT S.A.) at JRC laboratories. On the other hand, Rohde & Schwarz is developing the proper RF test equipment and laboratory environment for the antenna plus GNSS high precision receiver testing including the E6 bands. Once all these milestones succeed, a positioning field test with the MAGICA antenna will occur, obtaining relevant metrics and characterising how well the antenna system developed during this project.

For the MAGICA antenna design, the more relevant technical requirements are summarised in Table 1.

Results

The MAGICA antenna system presented in the paper consists of the following elements:

- The radiating element including the polariser circuit is responsible for antenna bandwidth, polarisation, radiation pattern, phase centre, multi-frequency characteristics.
- The RF front-end low noise amplifier (or RF front-end amplifier) with its frequency response defines frequency selectivity, noise factor, total antenna gain, phase centre stability, and complete antenna bandwidth.
- The housing is the plastic enclosure that protects the radiating element. Proper material selection to avoid any electrical influence on the antenna performance is required.

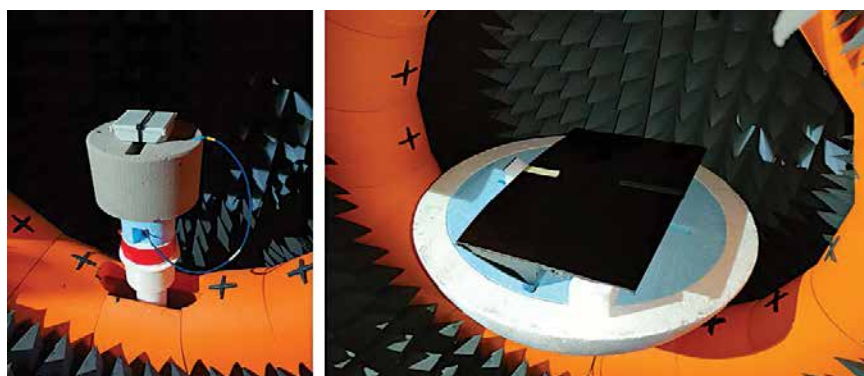


Figure 1: Radiating element inside the multi-probe system in an anechoic chamber for radiation pattern characterization in free space condition. Left picture: Antenna alone. Right picture: Antenna integrated in SEAT S.A. spoiler environment.

Each of the specific parts of the design has been simulated and optimised to get a feasible solution. The prototype of the MAGICA antenna has been manufactured and evaluated, and in the following subsections the relevant results of the prototype are presented showing: the performance of the radiating element, the performance of the RF front-end amplifier and the performance of the complete antenna system (in free space and in spoiler environment).

Table 1: MAGICA project technical requirements specification for the GNSS frequency bands.

Parameter	Requirement
Frequency bands	1164 - 1214 MHz (L5/E5a/E5b), 1260 - 1300 MHz (E6), 1559 - 1591 MHz (L1/E1)
Antenna Input Impedance	50 Ω
VSWR	2:1
Peak Realised Antenna Gain	> 2dBic at zenith
Axial Ratio at zenith	≤ 3 dB
GNSS Amplifier Gain	≥ 30 dB
Noise Figure (50 Ω)	≤ 3 dB
Phantom Supply Voltage	4.5 V - 5.5 V
Current Consumption	≤ 40 mA
Overall antenna dimensions	less than 100x100x30 mm

Measured results – Radiating element (without RF front-end amplifier)

The radiating element consists of a crossed IFA topology that covers the whole operating range. It has been prototyped using very thin metal sheets (0.5 mm) which offer a very low weight and a competitive antenna radiating element cost. The radiating element includes a polariser circuit to obtain the desired circular polarisation. The novel design of the radiation element offers very good performance covering all the

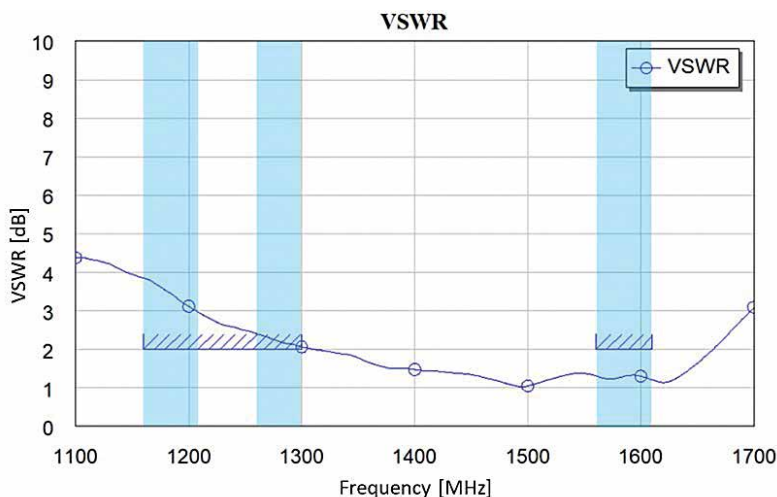


Figure 2: VSWR vs frequency of the radiating element of the MAGICA antenna including the polariser circuit

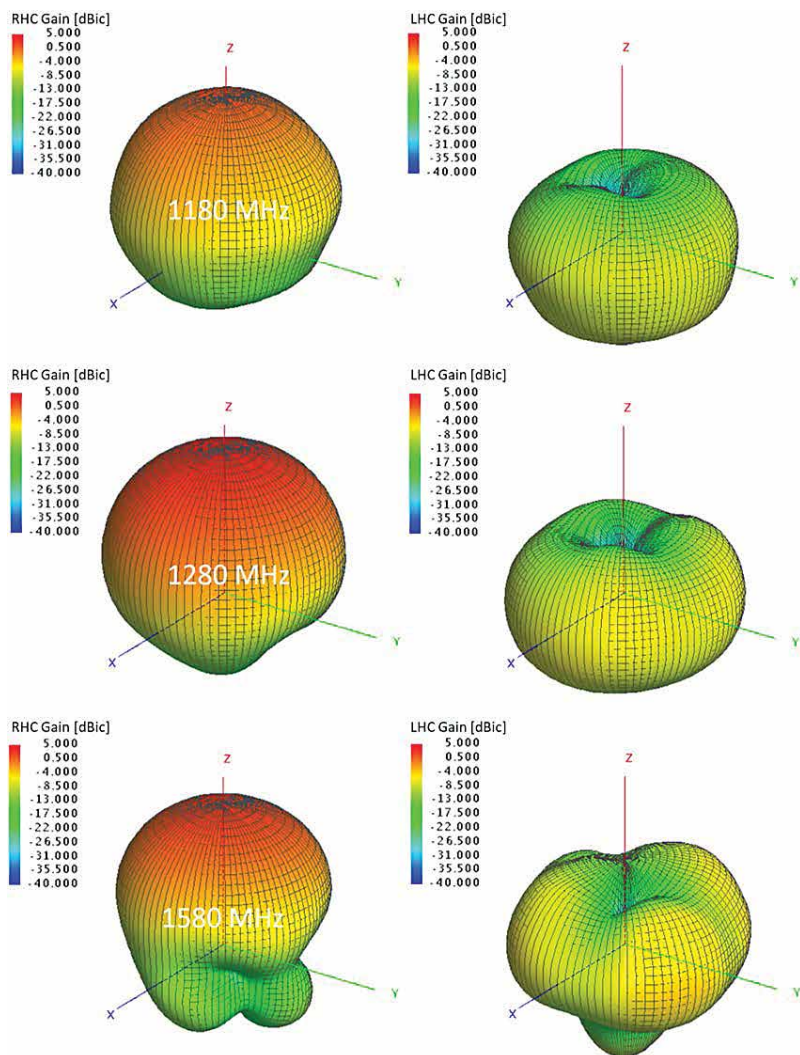


Figure 3: 3D RHCP and LHCP gain radiation patterns of the radiating element of the MAGICA antenna at 1180 MHz, 1280 MHz, 1580 MHz, including the polariser circuit

required bands (including E6) with a compact size of 80 x 80 x 20mm and can be integrated in any area free of metal without the need of any additional ground plane. In this section, the isolated radiating element is evaluated, as a first step to ensure an adequate performance of the whole active antenna system.

The relevant results of the measurements of the radiating element are described below, please note that the measurements include the polariser circuit. This polariser circuit is based on artificial transmission lines approach, i.e., right-handed and left-handed transmission line combination for little phase shift deviation along the required bandwidth.

One of the characteristics of the antenna is the VSWR (Voltage Standing Wave Ratio), which gives an idea on how efficiently the radiofrequency (RF) power is transmitted from the source to the antenna. Typically for optimal operation, low values of VSWR are desirable.

The highlighted regions correspond to the specific operating bands. As shown in Figure 2, this requirement is almost met in all the bandwidth of operation. It is specially met in the range 1559 - 1591 MHz (L1/E1) and very close to be met in the lower frequency bands, 1164 - 1214 MHz (L5/E5a/E5b), 1260 - 1300 MHz (E6). Some further adjustment with the prototype stage is on-going and with high confidence to be achieved.

The 3D right-hand circular polarised (RHCP) gain and left-hand circular polarised (LHCP) gain radiation patterns of the radiating element at three representative frequencies of the GNSS service (1180 MHz, 1280 MHz and 1580 MHz) have been measured. As shown in Figure 3, at zenith, the performance is purely RHCP with peak gain values from 2 to 4dBic (Figure 4) in almost all the bands of interest and with a strong rejection to LHC polarisation.

The axial ratio is the ratio between the semi major and semi minor axis of a circularly polarised antenna pattern. It is

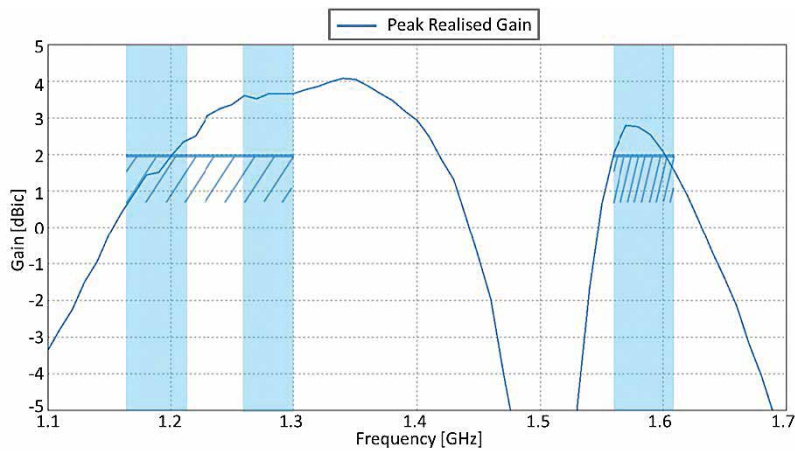


Figure 4: RHCP peak realised gain vs frequency of the radiating element of the MAGICA antenna including the polariser circuit

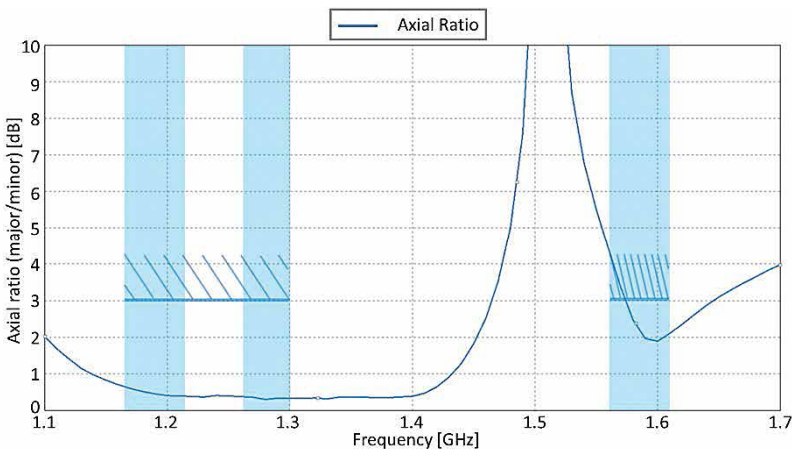


Figure 5: Axial ratio vs frequency at zenith ($\theta = 0$) of the radiating element of the MAGICA antenna including the polariser circuit

another important parameter for circularly polarised antennas. For an ideal circularly polarised antenna both values should be the same, so the ratio is equal to 0 dB. Actually, it is hard to achieve a good axial ratio across all the requested frequency bands of operation, but as shown in Figure 5, the axial ratio of the measured prototype is below 3 dB in practically all the operating bands, which is the typical requirement for GNSS antennas, and as well in the MAGICA project.

Measured results – RF front-end low noise amplifier

The next element to take into consideration for the antenna system is the RF front-end amplifier. It consists basically of an amplification and filtering stage. The following section describes the measurement results of the active stage for the prototype.

The results of the measurements of the specific parameters of the performance of the active part are listed in the tables below. For convenience, the requirement specification values are presented in the last column on the right of the tables.

The active elements are phantom powered through the connector and present a wide range of power supply operating DC voltage.

The relevant plots related to the RF front-end amplifier performance are illustrated below. Figure 6 shows its frequency response at the GNSS frequency bands of interest. The values in the figure make reference to the RF front-end amplifier transmission (S_{21}) and the reflection (S_{22}) coefficients. Note that the return loss and the reflection coefficient have the same magnitude when expressed in dB but opposite sign. The corresponding markers are placed on the previously stated GNSS bands. As shown in Table 3, the transference of power is above the specification, even though the reflection coefficient is not fully covering the targeted value. Additionally, an optimization loop is being carried out on the RF front-end amplifier output filter stage to improve this latter parameter.

Table 2: MAGICA antenna RF front-end amplifier DC summary performance table.

DC Specification	Measured values			Requirement
	Min.	Typ.	Max.	
Voltage (VCC) [V]	3		5.5	4.5 – 5.5
Current Consumption @ 5V [mA]		34		≤ 40
Power Consumption [mW]		170		≤ 200

Table 3: MAGICA antenna RF front-end amplifier performance summary table.

RF Specification (typ., 50 Ω)	Measured values				Requirement
	E5A/L5	E5B	E6	E1/L1	
Gain [dB]	30.2	30.5	30.25	30.4	≥ 30
Return Loss [dB] (at connector)	8.17	7	8.74	12.55	≥ 10
NF [dB] (room temp.)	< 1.7	< 1.7	< 1.7	1.5	≤ 3
GDR [ns] in-band	13.07	3.85	5.94	1.82	*
Stability (μ)	> 1	> 1	> 1	> 1	> 1
IP1dB [dBm]	-27	-27	-27	-27	-

* ~ 10ns in-band; ~ 50ns inter-band as maximum. Based on typical values of a commercial GNSS receiver for the automotive market

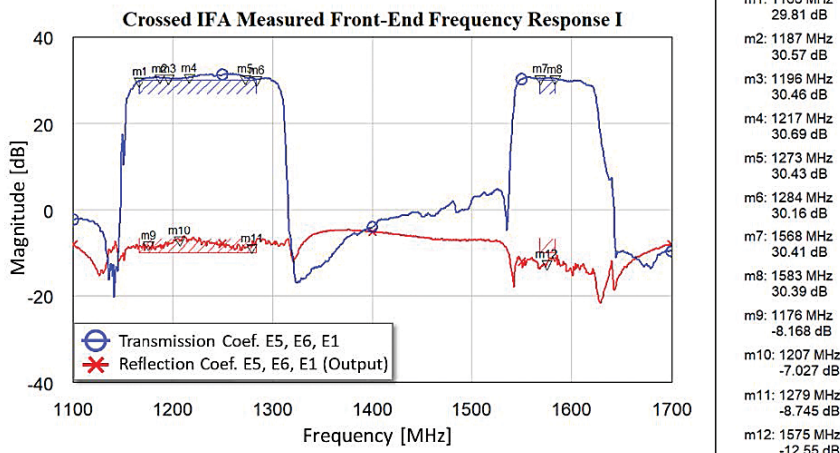


Figure 6: MAGICA antenna RF front-end amplifier transmission and reflection coefficients at the required GNSS frequency bands

On the other hand, the GDR at E5A/L5 band is slightly above the typical value of a commercial automotive GNSS receiver. This is due to the nature of the E5/L5, E6 SAW filter, since the significant bandwidth that is demanded is almost at the limit of the capabilities of this technology. Nonetheless, no degradation is expected as this only occurs at the lower edge of the band, where less energy of the signal is allocated.

On the evaluation of the RF front-end amplifier's response, one of the most relevant parameters is the noise figure. This parameter, together with the overall gain, gives an idea of the quality of the reception of the signals involved. Figure 7 shows the measured noise figure in the frequency bands of interest. This measurement, apart from the active components, includes the complete front-end circuit, with the frequency diplexer responsible for its frequency selectivity. It is important to note that the noise figure is below 3dB, which is the specific requirement defined in the project.

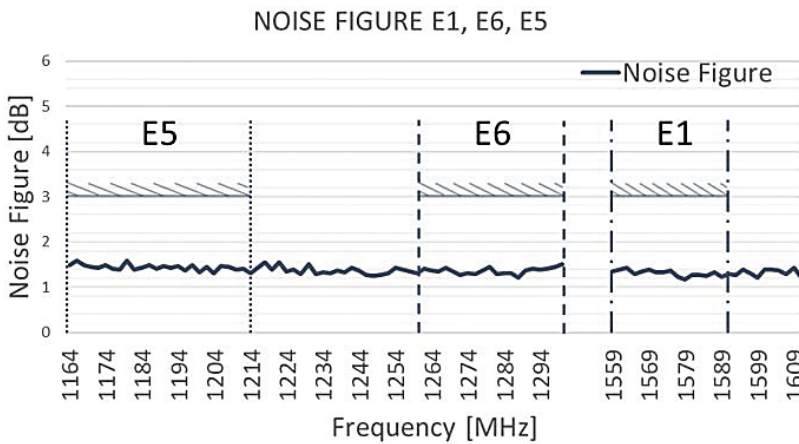


Figure 7: MAGICA antenna RF front-end amplifier noise figure at Galileo E1, E5, E6 frequency bands.

To minimise the error of the GNSS systems position and optimise the accuracy, the group delay ripple (GDR) of the RF front-end has to be controlled. The group delay ripple of the active part, Figure 8, shows a minimum delay either intra-band or inter-band.

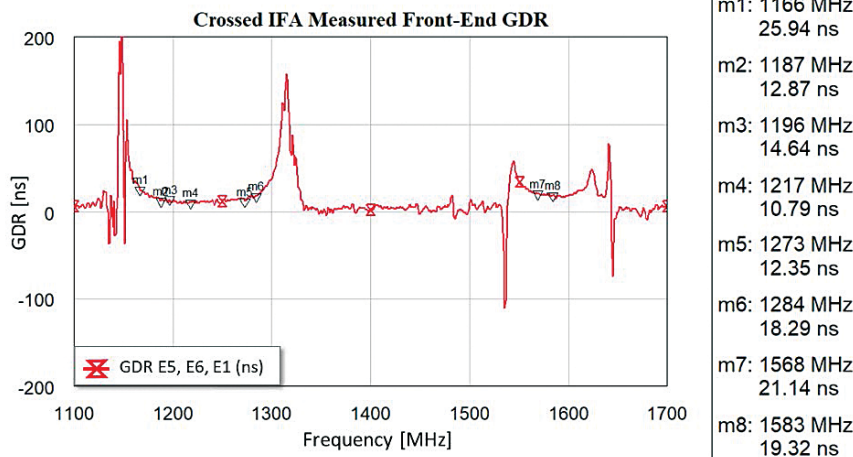
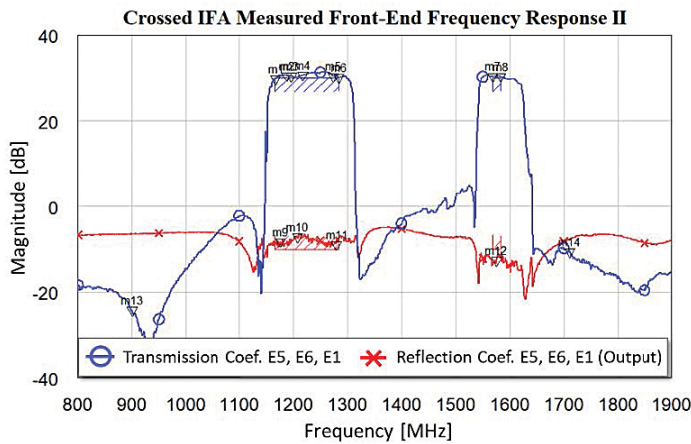


Figure 8: MAGICA antenna RF front-end amplifier group delay ripple at the required GNSS frequency bands

Despite not being a specific requirement inside the MAGICA project, the RF front-end amplifier should be capable of introducing a high level of rejection outside the operating bands. This is especially important in the case that the GNSS antenna is installed close to other antennas (i.e., telephony antenna, Wi-Fi antenna, ...). Figure 9 represents the frequency response of the RF front-end amplifier but also considers the rejection at the GSM telephony frequency bands. GSM telephony is the most critical source of interference to the GNSS service due to the high-power levels operated by these systems. As it shown in Figure 9, good rejection from possible interfering GSM systems is achieved with more than 10 dB at GSM 1800 MHz and 24 dB at GSM 900 MHz.



- m1: 1166 MHz
29.81 dB
- m2: 1187 MHz
30.57 dB
- m3: 1196 MHz
30.46 dB
- m4: 1217 MHz
30.69 dB
- m5: 1273 MHz
30.43 dB
- m6: 1284 MHz
30.16 dB
- m7: 1568 MHz
30.41 dB
- m8: 1583 MHz
30.39 dB
- m9: 1176 MHz
-8.168 dB
- m10: 1207 MHz
-7.027 dB
- m11: 1279 MHz
-8.745 dB
- m12: 1575 MHz
-12.55 dB
- m13: 900 MHz
-24.15 dB
- m14: 1710 MHz
-10.57 dB

was measured alone, the active 3D right-hand circular polarised (RHCP) gain and left-hand circular polarised (LHCP) gain radiation patterns of the active antenna prototype at three representative frequencies of the GNSS service (1180 MHz, 1280 MHz and 1580 MHz) have been characterised. The radiation pattern keeps the same shape as the passive antenna structure with a strong rejection of LHC polarisation, as shown in Figure 11, and with very good axial ratio performance (Figure 12). This latter fact leads to the expected peak gain values in the range of 32 to 34dBic.

Figure 9: MAGICA antenna RF front-end amplifier rejection at GSM telephony frequency bands

Table 4: MAGICA antenna RF front-end amplifier response at GSM telephony frequency bands.

RF Parameter at GSM (typ., 50 Ω)	900MHz	1800MHz
Rejection [dB]	24.15	10.6
IP1dB [dBm]	-16	-10

Measured results – Active antenna prototype in spoiler environment

After measuring the active prototype in free space condition, with promising results, it was time to begin with the integration process in the vehicle. After discussing possible locations in the vehicle with our consortium partner SEAT S.A., it was decided to place the antenna inside the plastic spoiler of the car, that is “invisible” from the RF point of view and therefore, providing good sky visibility in terms of GNSS signals. The spoiler area does not have any metallic structure, which might be an issue for other typical GNSS patch antennas that require a big ground plane underneath for optimal performance. The MAGICA antenna designed in the project does not have this problem as it is a standalone solution that doesn’t need any additional ground plane for optimal performance.

SEAT S.A. provided a vehicle spoiler where it was possible to install the antenna; this placement will be close to the final location in the car.

With the antenna located in the spoiler, it is possible to analyse the performance of the antenna considering the close vehicle environment and anticipate any effect that this can cause to the antenna.

The radiation pattern of the antenna has been measured, including the spoiler effects for three different and representative frequencies



Figure 10: MAGICA active antenna prototype antenna structure (left) and housing (right). Blurred image due to patenting study on-going.

Table 4 shows the measured values at the GSM telephony bands, as well as the 1 dB compression point at the input for these frequencies.

prototype is 89.3 x 89.3 x 29.2 mm. This compact design with reduced weight is attractive and feasible to be integrated in the vehicle.

Measured results – Active antenna prototype

Once the antenna radiating element and the RF front-end amplifier have been designed and characterised individually, it started the next phase of the project which is the characterization of the complete antenna system. The active antenna prototype consists of the radiating element together with the RF front-end low noise amplifier and the housing.

Figure 10 shows the MAGICA active antenna prototype including the radiating element, the RF front-end amplifier and a coaxial cable pigtail at the left side of the image, blurred, and the housing which is the enclosure of the prototype on the right side of the image.

The antenna prototype including the RF front-end amplifier has been measured in a multi-probe system anechoic chamber in free space condition (see Figure 1 – left).

The overall dimension of the active

In a similar way as the radiating element

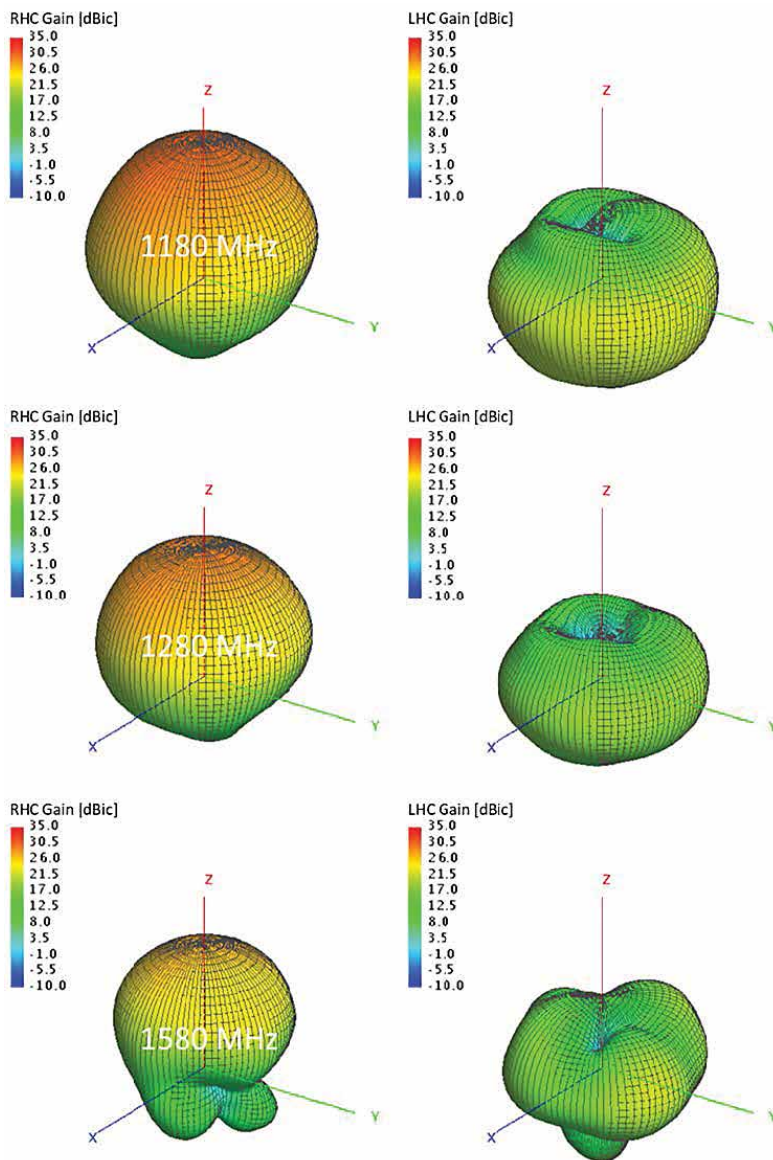


Figure 11: Active 3D RHCP and LHCP gain radiation patterns of the MAGICA antenna at 1180 MHz, 1280MHz, 1580 MHz

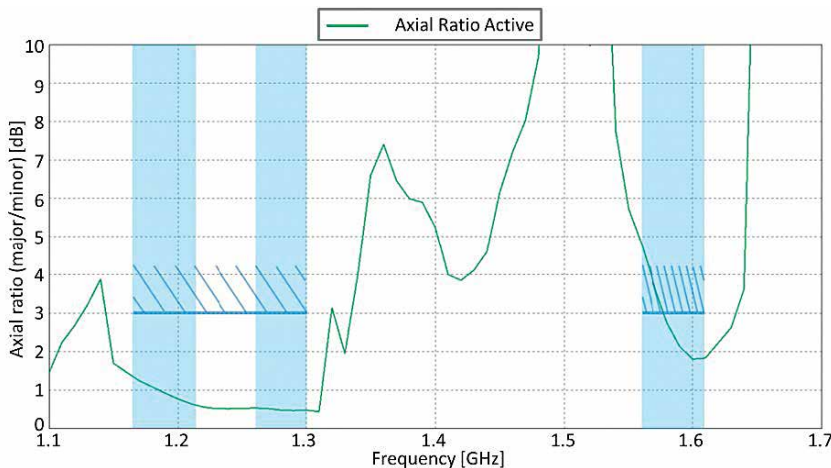


Figure 12: Axial ratio vs frequency at zenith ($\theta = 0$) of the active prototype of the MAGICA antenna

of the GNSS operating bands, as shown in Figure 1 – right.

It is important to notice that the shape of the radiation pattern is not distorted due to the spoiler effect keeping the expected and desired shape with peak gains pointing to the zenith and great discrimination of the LHC polarization (see Figure 13). The response of the antenna has been shifted down in frequency, as it was expected due to the dielectric and plastic effect, and the axial ratio of the integrated antenna now fits perfectly with the axial ratio requirement (see Figure 14).

The results of the measurements for the first prototype of the antenna system show an appropriate response of the system and they are in good agreement with the outcome from previous design steps, i.e., simulation results (see [8]).

Conclusions and next steps

The present paper shows the prototype results of the antenna designed in the scope of the MAGICA project providing a multi-constellation and multi-band (L1/E1, L5/E5 and E6) solution ready to be integrated in vehicles for high precision applications mainly needed for autonomous driving.

The radiating element has been designed using a novel metal sheets structure that leads to a cost effective and reduced weight solution providing the broadband frequency response for the desired operating bands, 1164 -1214 MHz (L5/E5a/E5b), 1260 - 1300 MHz (E6), 1559 - 1591 MHz (L1/E1).

To improve the antenna bandwidth and be able to cover all the required bands with a single element with RHC polarisation, a broadband polariser circuit based on the combination of left-handed and right-handed transmission line sections has been used.

The prototype has been measured in passive mode, achieving great RHCP gain values between 2 to 4 dBic in

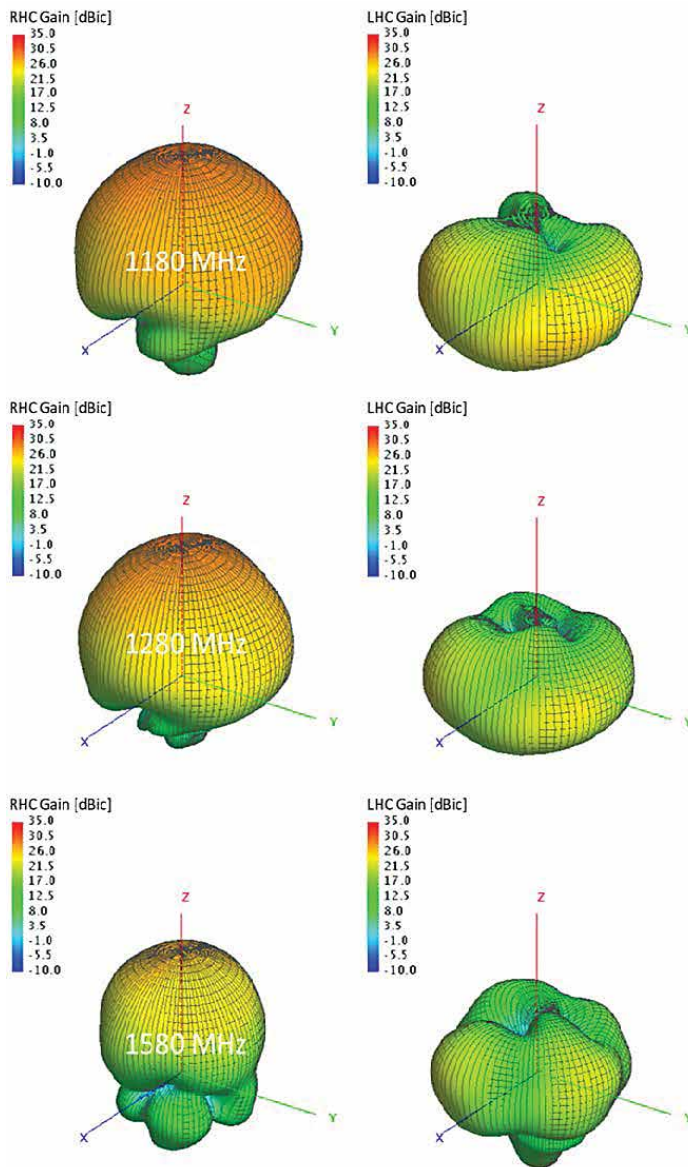


Figure 13: Active 3D RHCP and LHCP gain radiation patterns of the MAGICA antenna at 1180 MHz, 1280MHz, 1580 MHz installed in a piece of the spoiler environment

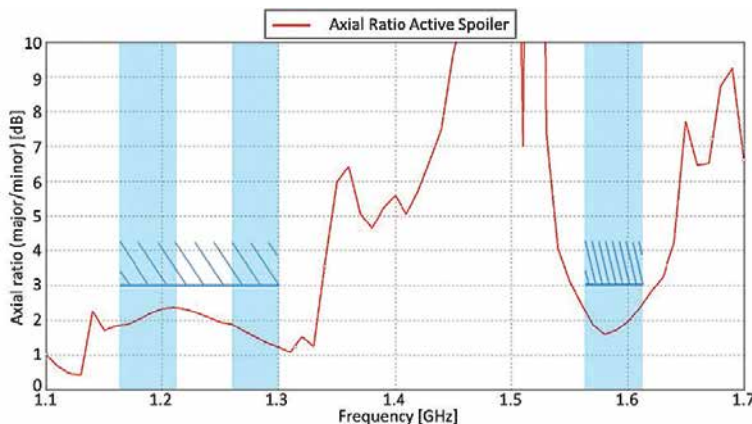


Figure 14: Axial ratio vs frequency at zenith ($\theta = 0$) of the active prototype of the MAGICA antenna installed in a piece of the spoiler environment

all the required bands and good axial ratio levels below 3dB in almost all the desired frequency ranges. The RF front-end amplifier has been designed and adjusted in order to meet the broadband frequency response, achieving gains of 30 dB with low noise figure values below 2dB in all the frequency bands and with a low group delay dispersion.

The RF front-end amplifier design has been integrated with the radiating element in order to obtain the complete active antenna system.

The novel design developed in the project offers a high-performance compact antenna that can be used as a standalone solution because it does not require an additional ground plane for optimal performance. This gives a significant advantage as it can be installed in vehicle positions where large ground plane structures are not available.

After discussions with SEAT S.A., the spoiler area of the vehicle was selected as a good integration location for the GNSS antenna, to avoid any visual impact on the vehicle aesthetics, therefore the antenna design was optimised for this location. Measurements of the complete active antenna system integrated into the SEAT S.A. spoiler show good performance fulfilling the required antenna technical goals.

As it can be confirmed, the results are very promising, fulfilling the requirements needed for this kind of application. Small adjustments will be needed regarding the integration of the antenna in the housing and in the car structure. Indeed, this is one of the challenges of the project, the integration in a real vehicle model with limited space for the location of the antenna should not lead to a degradation of the performance of the design. The multi-band, multi-constellation GNSS antenna developed will be a feasible solution ready for the autonomous vehicle.

The way forward of the MAGICA antenna design will be focused on the analysis of the influence of the car structure in the radiation pattern of the integrated

Dubai opens world's largest solar-powered data centre

Dubai has inaugurated the largest solar-powered data centre in the world at the Mohammed bin Rashid Al Maktoum Solar Park in the emirate. The centre is operated by the Moro Hub, a wholly owned subsidiary of the Dubai Electricity & Water Authority (Dewa).

It is designed to provide next-generation services in the areas of digital transformation, cloud and hosting services, cybersecurity, smart cities, internet of things (IoT) services and professional and managed services, as well as Moro services supported by ChatGPT technology.

The data centre also supports the Dubai Clean Energy Strategy 2050 and the Dubai Net Zero Emissions Strategy 2050 to generate 100 per cent of its energy production capacity from clean energy sources by 2050. The centre uses latest developments in the area of internet of things (IoT), cybersecurity, digital twins, artificial intelligence (AI), cyber recovery-as-a-service, network-as-a-service as well as the Moro Open Cloud. <https://gulfbusiness.com>

Siemens partners with Swinburne University

Siemens and Swinburne University of Technology have agreed to set up the most advanced future Energy Transition Hub of its kind in Australia in at the University's Hawthorn campus in Melbourne. The \$5.2 million Hub aims to build a future energy grid laboratory accessible to students and industry. When fully operational, it will also offer researchers and industry the opportunity to work on solutions for greener, more efficient future energy systems. The Hub will enable users to leverage digital twins of energy grids, map scenarios, research new findings, develop original and creative hypotheses, and test results. It will be home to a digital twin of Australia's energy grid that commercial research teams can use to run simulations of new, innovative solutions and software. [siemens.com](https://www.siemens.com)

antenna design. The efforts will be focused together with the mechanical engineers on the manufacturing and the proper integration in the vehicle without a substantial degradation of the performance.

The proposed prototype antenna solution will be measured at vehicle level in a 3D anechoic chamber integrated in an actual SEAT S.A. vehicle model and system level tests including laboratory and field tests in several urban and rural areas will be performed.

This will be the closest case to that of a real scenario, in order to achieve a design ready for the mass-production stage.

Further information of the project could be followed through the website: www.gnss-magica.eu.

Acknowledgements

This work is supported by the EUSPA under the European Union's Fundamental Elements research and development program under grant agreement No. GSA/GRANT/01/2018.

References

- [1] Autonomous Vehicles: Timeline, <https://www.roadtraffic-technology.com/comment/autonomous-vehicles-timeline/>, last accessed 2022/04/06
- [2] Automated Driving – Challenges in Simulation, <https://www.frost.com/frost-perspectives/automated-driving-challenges/>, last accessed 2022/04/06
- [3] Pan L., Cai C., Zhu J. and Cui X.: Kinematic Absolute Positioning with Quad-Constellation GNSS. In (Ed.), Kinematics - Analysis and Applications. IntechOpen (2019).

- [4] Leica AR25 GNSS Antenna. <https://leica-geosystems.com/products/gnss-reference-networks/antennas/leica-ar25>, last accessed 2022/05/10
- [5] Trimble GNSS Ti-V2 Choke Ring Geodetic Antenna. URL: <https://www.trimble.com/Real-Time-Networks/Trimble-Choke-Ring-Antenna.aspx>, last accessed 2022/05/10
- [6] InPAQ Technologies GPS Antenna Manufacturer. URL: <https://www.inpaqgp.com/index.php>, last accessed 2022/05/10
- [7] Amotech Antenna Solution. URL: http://global.amotech.co.kr/wp/antenna-solution_2/, last accessed 2022/05/10
- [8] Filatov, E., Vélez, M.A., Gemio, J., Vicente, J.J., Capdevila, R., Tantinyà, L., Gil, A., Cardala, A., Baños, D., Mogas, P., Reyes, J.: MAGICA project: Development of a Multi-frequency Automotive GNSS Integrated Cost effective Antenna. In: WiP Proceedings of the International Conference on Localization and GNSS (ICL-GNSS 2021)
- [9] Precise positioning for autonomous vehicles. <https://www.controleng.com/articles/precise-positioning-for-autonomous-vehicles/>, last accessed 2022/04/06

The paper presented in ICL-GNSS 2022 WiP, June 07–09, 2022, Tampere, Finland was originally published in CEUR Workshop Proceedings (CEUR-WS.org) Proceedings.

© 2022 Copyright for this paper by its authors.

Use permitted under Creative Commons License Attribution 4.0 International (CC BY 4.0).

The paper is republished with authors' permission. 

UN agreement on protecting marine biodiversity

After years of negotiations, the member states of the United Nations have finally reached an agreement on the conservation of biodiversity in the oceans. The High Seas Treaty must protect international waters, which make up about two thirds of the ocean surface.

Two thirds of the oceans lie outside countries' exclusive economic zones and belong to the high seas. These are largely areas outside national jurisdiction. While the good health of marine ecosystems is critical to life on Earth, only 1% are currently protected. The agreement aims to change that and is seen as essential to achieving the goal agreed in December to protect 30% of the world's land and sea by 2030.

In seven years' time, 30% of that open sea must therefore be protected so that underwater life is preserved and can also recover. It is essential that fishing, shipping and deep-sea mining are restricted in these protected areas. The 'historic treaty' also contains agreements on comprehensive environmental impact assessments. This includes aspects from acidification to underwater noise to overfishing to pollution. The treaty will allow a single ecosystem approach to be taken that collectively covers all these issues. <https://news.un.org>

Royal Navy enters the Metaverse

The Royal Navy is embracing Virtual Reality to train sailors of tomorrow in cutting-edge new navigation simulators. Sailors will don headsets to take them into a naval 'metaverse' immersing them in key – and sometimes dangerous – manoeuvres, all from the safety of a naval base.

The VR headsets will be just one facet of new state-of-the-art replica ship's bridges, with software capable of recreating the entire fleet, harbours and waters around the globe, and challenging weather conditions by day and night. www.royalnavy.mod.uk 

Galileo signal component tested for Internet of Things use

One of Europe's Galileo satellites has been reconfigured to emit a new signal component optimised to serve low-end receiver devices and Internet of Things applications.

The metre-level accuracy provided by Galileo's Open Service makes it the world's most accurate generally-available service, out-performing other global navigation systems such as GPS and providing not only positioning, navigation and timing services to users worldwide, but also aiding rescue missions. Yet individual satellites within the constellation can also be used to trial new signals and services as the system continues to progress.

Embedded sensors placed in everything from home appliances to farm equipment to smart city infrastructure are on the way, allowing such items to report and exchange their location information so they can work together. At the same time, these stand-alone sensors are constrained by strict limits on available battery power and computational resources.

To serve this emerging market of IoT and snapshot devices, and to respond to the needs of chipset manufacturers, Galileo engineers looked into requiring a positioning signal that can be acquired with lower computational complexity. www.esa.int

ACSER upgrades satellite receiver for new applications

The University of New South Wales has produced an advanced satellite receiver that accepts GPS and Galileo signals. This locally developed technology could play an important role in Australia's space future.

This receiver accepts signals from two satellite systems, GPS and Galileo, across multiple frequencies. The Australian Space Agency provided funding via the International Space Investment initiative.

Professor Andrew Dempster, Director of the Australian Centre for Space Engineering Research (ACSER) at the University of New South Wales, led the development of the receiver.

The end product is an advanced receiver capable of Global Navigation Satellite System (GNSS) reflectometry. This is a remote sensing technique where signals are reflected from the Earth's surface to study environmental conditions over land and sea, such as floods and storms. www.industry.gov.au

NASA Moon Mission set to break record in navigation signal test

As the Artemis missions journey to the Moon and NASA plans for the long voyage to Mars, new navigation capabilities will be key to science, discovery, and human exploration.

Through NASA's Commercial Lunar Payload Services initiative, Firefly Aerospace of Cedar Park, Texas, will deliver an experimental payload to the Moon's Mare Crisium basin. NASA's Lunar GNSS Receiver Experiment (LuGRE) payload will test a powerful new lunar navigation capability using Earth's GNSS signals at the Moon for the first time.

LuGRE — developed in partnership with the Italian Space Agency (ASI) — will receive signals from both GPS and the European GNSS constellation, Galileo, and use them to calculate the first-ever GNSS location fixes in transit to the Moon and on the lunar surface. The LuGRE mission will use a specialized weak-signal receiver developed by Qascom, an Italian company specializing in space cybersecurity and satellite navigation security solutions, and funded by ASI. www.nasa.gov

Indian Railways ties up with ISRO for real-time train tracking

The Indian Railways is harnessing the power of data analytics for integrated transportation. It has commenced a project which will now enable real time

tracking of train movements with the assistance of satellite imagery under the Real Time Train Information System (RTIS) project. D.K. Singh, Managing Director, Centre for Railway Information Systems (CRIS), said that CRIS has collaborated with Indian Space Research Organization (ISRO) for live tracking to help Railways run trains efficiently.

ISRO has developed its own regional navigation satellite system called Navigation with Indian Constellation (NavIC) and Bhuvan, a web-based utility which allows users to explore a set of map-based content being deployed for tracking. “We have taken bandwidth from ISRO and integrated our systems with NavIC and Bhuvan. Every locomotive is fitted with a device and SIM, which communicates the train’s real position to the satellite and feedback is received. The movement is updated every three seconds. Until now, 4,000 locomotives have been installed with the technology, and new locomotives that are being manufactured come pre-installed with the tracking devices,” Mr. Singh said.

The CRIS has now developed a hand-held device that can help reduce queues by providing tickets on platforms to unreserved passengers. Mr. Singh said that the CRIS has identified 90 use cases where AI can be used for improving Railways services, including seat allocation, prediction analysis on when freight trains will be emptied, and balancing stocks of medicines across the Railways health infrastructure www.thehindu.com

Orolia releases Skydel 22.12 GNSS simulation software

Orolia’s Skydel GNSS simulation software, can now generate more than 500 simulated satellite signals. This platform is suitable for GNSS users, experts and manufacturers, as well as users needing a low-Earth-orbit-capable simulation system. It contains a feature that includes multi-constellation and multi-frequency signal generation, remote control from user-defined scripts, and integrated interference generation. www.orolia.com 

EagleView launches next-gen Asset Management with AI

EagleView announced the launch of its next-generation asset management solutions. Combining high-resolution oblique aerial imagery with machine learning, it is solving a variety of asset management challenges for local governments and commercial organizations. www.eagleview.com

Thales and LuxCarta to offer AI solutions

Thales and LuxCarta join forces to offer artificial intelligence (AI) enhanced solutions for intelligence and military cartography. Thales has a recognized expertise in the production of military and intelligence maps with a detailed knowledge of the technical references specific to the military sector. The Group supports the armed forces by creating accurate and reliable maps from satellite images that are scanned and vectorized. LuxCarta is at the forefront of the field of AI in deriving geospatial products thanks to its BrightEarth platform and associated technologies. For intelligence and military geography, AI is particularly useful in photo interpretation. www.thalesgroup.com

ISS opens technology advancement research

The International Space Station (ISS) National Laboratory released a new research announcement soliciting flight concepts for “Technology Advancement and Applied Research Leveraging the ISS National Lab.”

This solicitation is open to a broad range of technology areas including chemical and material synthesis in space, bonding, translational medicine, in-space edge computing and on-demand cloud computing technologies, and the use of ISS remote sensing data to improve geospatial analytics for commercial use.

Space-based technology development and demonstration is a strategic priority for the ISS National Lab, as it provides an

opportunity for accelerated technology maturation to enable advancements that improve life on Earth and build commerce in low Earth orbit.

Through this research announcement, offerors may propose to use the unique ISS environment to develop, test, or mature products and processes that have a demonstrated potential to produce near-term and positive direct or indirect economic impact. www.ISSNationalLab.org

ISRO receives Indo-US jointly developed NISAR satellite

The Indian Space Research Organisation (ISRO) received the NASA-ISRO SAR (NISAR) satellite from the U.S. space agency in Bengaluru. NISAR is a Low Earth Orbit observatory jointly developed by NASA and ISRO.

The Space Mission is part of India-US civil space collaboration. NISAR with the largest ever radar antenna, 12 meters long drum shaped, wire mesh reflector extended from a 30 foot boom, is the most advanced radar system that will study natural hazards, melting sea ice, and groundwater supply.

Ubotica slashes satellite data overload with on-board AI solution

Ubotica Technologies announced the CogniSAT-CRC solution which maximises Earth Observation asset utilisation using flight proven CogniSAT technology. Using state of the art lossless image compression, and a flight-proven AI-based Cloud Detection and Removal algorithm, CogniSAT-CRC delivers at least a six-fold increase in useful data capture per orbit for Earth Observation (EO) satellites thereby maximising the areas of interest scanned during each orbit.

CogniSAT-CRC comes in a mechanical and power envelope compatible with small satellites, even down to CubeSats, and maximises the utilisation of EO assets by eliminating the impact of downlink data bottlenecks. <https://ubotica.com> 

NYPA receives FAA waiver for automated drone operations

The New York Power Authority (NYPA) has received its first federal approval to fly unmanned aircraft systems (UAS) or drones beyond the visual line of sight (BVLOS) of the pilot in command. In a significant step forward, this Federal Aviation Administration (FAA) waiver enables NYPA to conduct fully remote drone operations such as asset and vegetative management inspections at its Blenheim-Gilboa Pumped Storage Power Project in Schoharie County. NYPA's growing drone program supports its industry-leading asset management strategies and is part of an Authority-wide digitization initiative to modernize grid infrastructure to advance the efficient delivery of clean power statewide. www.nypa.gov

XAG and Chia Tai to launch agricultural drones in Thailand

XAG has teamed up with FarmInno (Thailand) by Chia Tai Group, Thailand's agricultural company, to introduce fully autonomous agricultural drones in Thailand. This takes smart agriculture to the next level aiming to scale up the potential of Thai farmers with advanced technology and increase both productivity and quality in the agricultural sector. The drones are fully autonomous and powered by AI, making them highly efficient in terms of spreading and precision spraying. www.xa.com

New partnership on drone cell tower inspection

Optelos, the supplier of visual data management and analysis software for cell tower inspection applications and Pathwave, the provider of safety and job closeout software for telecom crews, announced the technology partnership. The partnership will allow carriers, asset owners and contractors to combine the latest drone data captures and digital twins with safety compliance and closeout data to automate and

better document the complete tower inspection process. <https://optelos.com>

DroneUp partners with McMillon Innovation Studio

The McMillon Innovation Studio has partnered with DroneUp, LLC to evaluate opportunities to expand DroneUp's operations, including on college campuses. It offers an opportunity for student design and product teams to develop human-centered design solutions to problem statements that have social impacts. The studio serves students across campus and a variety of other industry partners.

The Studio will collaborate with DroneUp on a design team project focused on campus safety and security. The design team will coordinate with key stakeholders on campus to discuss possibilities that could become innovative solutions to real-world problems, and they will also evaluate legal and policy aspects around privacy and safety. <https://news.uark.edu>

Drone automation and public safety

Skyfire Consulting have announced its strategic partnership with VOTIX — maker of pioneering drone automation. This strategic partnership will allow VOTIX to leverage Skyfire's decade of experience within public safety and to provide agencies a smoother path towards starting and operating Drone First Responder (DFR) programs. <https://votix.com>

D-Fend Solutions and Securiton partnership

D-Fend Solutions and Securiton Germany, a system provider, integrator and specialist in security systems, have signed a partnership agreement. Through this partnership, D-Fend Solutions will provide the EnforceAir system, its market-leading flagship technology, for which it carries out research, development, and innovation. D-FendSolutions.com

Rohde & Schwarz launches drone based analyzer

Rohde & Schwarz will launch its R&S EVSD1000 VHF/UHF nav/drone analyzer. The analyzer provides accurate and efficient drone inspection of terrestrial navigation and communications systems along with outstanding accuracy and the measurement repeatability customers need.

The analyzer is a signal level and modulation analyzer for medium-sized drones. It is the only instrument that combines measurements of instrument landing systems (ILS), ground-based augmentation systems (GBAS) and VHF omnirange (VOR) ground stations in a single box. The mechanical and electrical design is optimized for drone-based, real-time measurements of terrestrial navigation systems with up to 100 measurement data sets per second. www.rohde-schwarz.com

BRINC to release LEMUR 2 drone

BRINC, an American developer and manufacturer of technology in the service of public safety, has announced the release of its next-generation drone, LEMUR 2, which is the latest product from BRINC and is specially designed to enable law enforcement and public safety professionals to survey areas too dangerous to send a person, assess a threat profile, and de-escalate conflict without putting individuals in harm's way. www.dronerds.com

Hackerwatches launches HackerMini Drone

Hackerwatches has launched the HackerMini Drone. It is packed with advanced features to enhance the aerial experience for both beginners and professionals. It is a powerful mini drone that can capture 4K HD video and snap photos with the simple gesture of your hand. The drone ensures smooth and stable flights, allowing you to focus on capturing the perfect shot. www.hackerwatches.com 

Mercedes-Benz and Google strategic partnership

Mercedes-Benz and Google announced a long-term strategic partnership to further accelerate auto innovation and create the industry's next-generation digital luxury car experience. With this partnership, Mercedes-Benz will be the first automaker to build its own branded navigation experience based on new in-car data and navigation capabilities from Google Maps Platform. <https://group.mercedes-benz.com>

EH216 AAV completes its Japan's first passenger-carrying demo flight

EHang Holdings Limited has announced that its EH216 passenger-grade autonomous aerial vehicle (AAV) has completed its first passenger-carrying autonomous flight demonstration within Japan, which also marks the first passenger-carrying flight for an autonomous eVTOL aircraft in Japan.

Earlier in July 2022, EH216 completed Japan's first eVTOL point-to-point demo flight for air mobility in Oita City, Oita Prefecture, making a breakthrough in exploring UAM use cases in Japan. This year, EHang and its partner, MASC, revisited Oita to demonstrate the EH216's first passenger-carrying autonomous flight within Japan, which is expected to further enhance the awareness and interest of UAM in the local community and accelerate the development of the Japanese UAM industry. www.ehang.com

TEOCO expands 5G geolocation analytics and optimization

TEOCO, a provider of analytics, assurance, planning and optimization solutions to over 300 communication service providers (CSPs) worldwide, released a new version of its Mentor Suite. This latest release, v2022.2, includes enhancements to Mentor's Server, Client and CogniSense products to expand the breadth of analytics use cases with a particular focus on 5G geo-analytics and optimization using advanced machine learning algorithms. www.teoco.com

Radisys introduces ReachPoint Indoor Navigation

Radisys Corporation announced the availability of Radisys ReachPoint, a network-based geolocation platform that allows Mobile Network Operators (MNOs) to deliver real-time geolocation service capable of reaching places where GPS may not be available. The solution enables Enterprises to get the location of any connected device without relying on GPS, using geospatial data from cell towers and Wi-Fi nodes. radisys.com

Aurrigo International partners with Changi Airport

Singapore's Changi Airport Group (CAG) is partnering with autonomous shuttle specialist Aurrigo International for the continued joint development and testing of advanced autonomous, electric baggage vehicles.

The multi-year partnership with CAG provides an opportunity for the further development of Aurrigo's autonomous solutions at Changi Airport and demonstrations to showcase the technology to other airports and stakeholders. www.airport-technology.com

SOLiTHOR and Sonaca sign new MoU

The Belgian solid-state Lithium battery technology company, SOLiTHOR and the leading aerospace company, Sonaca, have signed a bilateral Memorandum of Understanding to go into partnership where they will jointly develop safe, high-density rechargeable solid-state Lithium battery systems for Regional Aircraft and Urban Air Mobility. This partnership will also expand to Satellite systems as well as Defence systems. www.solithor.com

Ooredoo Group selects Nokia to deploy 5G

Nokia announced that it has been selected by Ooredoo Group to upgrade its existing radio access networks (RAN), as well as deploy new sites in Algeria and Tunisia. This will improve the

network performance and help Ooredoo Group to prepare for a launch of 5G services in the future. www.nokia.com

WiMi explores 6G holographic communication

WiMi Hologram Cloud Inc. has announced an in-depth study on the integration of edge computing, robotics, artificial intelligence, digital holography, and 6G communications using 6G high-speed broadband networks in combination with its self-developed multi-dimensional holographic vision mapping technology. The holographic communication service is a holistic application solution for the acquisition, encoding, transmission, rendering, and display of data from highly immersive, multi-dimensional interactive application scenes based on naked-eye holographic technology, encompassing the entire end-to-end process from data acquisition to multi-dimensional sensory data restoration, and is a highly immersive, highly natural interactive business form. <http://ir.wimiar.com>

Nokia and Bosch set a new bar for 5G positioning

Nokia and Bosch have jointly developed 5G-based precision positioning technology intended for new Industry 4.0 use cases. The two have deployed the proof of concept in a Bosch production plant in Germany, where extensive tests under realistic manufacturing conditions have shown an accuracy within 50 cm in 90 percent of the factory footprint.

The positioning technology tracks mobile and portable devices connected to the 5G network, accurately determining their positions where no global navigation satellite service coverage is available, for instance in factories, warehouses or underground facilities. As part of the factory test, an enhanced private 5G network was able to determine the precise position of assets such as automated guided vehicles (AGVs), mobile robots and mobile control panels – tracking their movements throughout the plant in real time. www.nokia.com 

Trimble announces advanced path planning technology

Trimble has announced its new advanced path planning technology. This software-based technology gives its end users and equipment manufacturers the ability to optimize and automate the trajectory, speed and overall path design of industrial equipment to increase efficiency of work. This new software capability will enable a broad range of autonomous applications across a variety of industries, including construction and agriculture. www.trimble.com

ecNation RV and Boat Storage links up with WhereSafe GPS

RecNation Storage, operator and developer of specialized recreational vehicles and marine storage facilities, announced the launch of RecNation Rental. It has selected WhereSafe GPS as a vendor partner to offer its RV renters real-time GPS tracking as a value-added service for its RV renters. www.wheresafe.com

Eurosense relies on Vexcel Imaging and RhinoTerrain for LOD 2 city models

Eurosense has achieved outstanding results in creating high-quality watertight building models of Old Town Graz, Austria, at Level of Detail (LOD) 1 and 2. The particular project scope included images from Vexcel's UltraCam Osprey 4.1 at 80% forward and 60% sideward overlap and 5 cm Ground Sampling Distance. Image post-processing and Aerial Triangulation of both nadir and oblique imagery was done within UltraMap. The resulting Exterior Orientations and TIFFs were imported into RhinoCapture for digitizing vectors in a 3D stereographic environment provided by DAT/EM's Summit Evolution. vexcel-imaging.com

Antenova's ultra-small high precision GNSS module

Antenova Ltd's latest compact high precision GNSS module is GNSSNova M20072, which is a GNSS receiver

with integrated GNSS antenna and greatly reduced power consumption. It uses a MediaTek 12nm low energy chip with 1.8V power supply which uses 70% less power than older chipsets. The power consumption of the module can therefore be as low as 21mW for a GPS fitness tracker, and GNSS-enabled products built with the M20072 will have a longer battery life. www.antenova.com

CHC Navigation releases GNSS RTK steering system

CHC Navigation has released the NX510 SE Auto-Steer, an automated steering system that retrofits several types of new and old farm tractors and other vehicles. It can be connected to local real-time kinematic (RTK) networks or GNSS RTK base stations.

NX510 SE is a guidance controller powered by multiple corrections sources and five satellite constellations: GPS, GLONASS, Galileo, BeiDou and QZSS. It has a built-in 4G and UHF modem that connects to all industry-standard differential GPS and RTK corrections to achieve centimeter-accuracy steering. <https://chcnv.com>

TCarta Expands Role in Seabed 2030 Ocean Survey Project

TCarta Marine, a global provider of hydrosatial products and services, has expanded its role in the Seabed 2030 project that seeks to map the entire ocean floor by 2030. Having already directly contributed extensive satellite-derived bathymetry (SDB) to the endeavor, TCarta has developed capacity building initiatives to train international hydrographic offices in creating their own SDB data sets for Seabed 2030 and other applications. www.tcarta.com

GMV to increase Europe's maritime surveillance capabilities

GMV has secured a contract from the European Defence Agency (EDA) to develop the new software

applications of the third phase of MARSUR (MARSURIII).

At the end of 2005, European leaders agreed to launch a project devoted to maritime surveillance (MARSUR) through EDA, with the aim of creating a European network that would link together existing national systems. Common standards were needed to ensure maritime safety and security, as the European Union has more than 14,500,000 km² of sea area under its remit, over which around 12,000 vessels sail every day.

Since its inception, MARSUR's capacity has evolved through different phases to integrate various technological improvements. While the previous phase of the project (MARSUR II) focused on network maintenance and updating MEXS, the software that ensures the automatic exchange of maritime surveillance data between participating countries, MARSURIII will upgrade the MEXS and user interface (MUI) technology, enable the exchange of restricted information, and improve the system's interoperability with other maritime security networks, mainly with the EU's Common Information Sharing Environment (CISE).

The overall objective is to improve the operational use of MARSUR in maritime missions and operations carried out under the EU's Common Security and Defense Policy (CSDP), the policy framework through which Member States are developing a strategic security and defense culture in Europe to preserve and strengthen international security. www.gmv.com

NV5 Geospatial to analyze climate change

NV5 Geospatial, announced that it will conduct aerial lidar and orthoimagery surveys across the Caribbean on behalf of the Caribbean Community Climate Change Centre (CCCCC).

Funded by the Caribbean Development Bank (CDB), this pilot project will provide advanced geospatial data to help the island nations better understand natural

and man-induced climate changes and develop programs to support resilience and sustainable development, and establish a foundation for future work. The project is complex, covering 10 sites spread across more than 3,000 kilometers, with mostly ocean between them. www.nv5.com

GEODNET announces GNSS corrections service

GEODNET has announced initial availability of a Real-Time Kinematic (RTK), Centimeter Precision, GNSS Corrections Service for Original Equipment Manufacturers (OEMs) and Systems Integrators. It is compatible with thousands of fielded GNSS receivers from all major brands, on-vehicle automated steering and spraying kits, as well as the latest drones and robots. geodnet.com

Optimized LTE CAT 1 bis module SIM7672x Series

SIMCom has launched the optimized LTE Cat.1 bis module the SIM7672X Series, delivering an all-encompassing solution that offers a new generation of fast, powerful, high-performance IoT connectivity with global network coverage, lower costs, smaller form factor, and higher power efficiency. www.simcom.com

ComNav Tech Launches GNSS receiver

ComNav Technology has introduced a new product called Venus Laser RTK, which allows positioning without the need for a range pole.

For the prism-free total station, the principle behind this technology is that the laser beamer on the total station sends a laser pulse towards an object and measures the time taken for the pulse to be reflected off the object and returned to the transmitter. This enables the distance between the transmitter and object, as well as the coordinates of the object, to be determined. The Venus Laser RTK GNSS receiver is equipped with a centimetre-level laser rangefinder on the bottom, with which it determines the distance

between the RTK and the object. It can obtain centimetre-level positioning results through the CORS network. Furthermore, the IMU sensor allows tilt compensation within 60° tilt, making it easy to obtain accurate coordinates. comnavtech.com

STMicroelectronics reveals NB-IoT industrial modules

STMicroelectronics' ST87M01 ultra-compact and low-power modules combine highly reliable and robust NB-IoT data communication with accurate and resilient GNSS geo-location capability for IoT devices and assets. The fully programmable, certified LTE Cat NB2 NB-IoT industrial modules cover worldwide cellular frequency bands and integrate advanced security features. www.st.com

Esri signs agreement with Malta

Malta Information Technology Agency (MITA) has signed an enterprise agreement with Esri to specifically enhance MITA's GIS capabilities. The three-year agreement will provide Esri software, professional services, and technical support to MITA and 22 other agencies across the Maltese government. The agreement will enable existing GIS users in Malta, including agencies for planning, public works, and transportation, to enhance their activities and services with the latest geospatial capabilities from Esri. www.esri.com

Quectel GNSS module LC76G

The LC76G module is a compact, single-band, ultra-low power GNSS module that features fast and accurate location performance. The module can concurrently receive and process signals from all satellite constellations including GPS, GLONASS, BeiDou, Galileo and QZSS thereby maximizing the number of satellites visible to a device. quectel.com

New Mil Spec GPS/GNSS antennas

Pasternack recently introduced an innovative series of mil-spec GPS/GNSS antennas for use in various small

form factor and mobile applications. The antennas are engineered for environmental performance according to the MIL-STD-810G standard and include multi-standard GPS L1, GALLILEO E1 and GLONASS options. These antennas feature linear polarization for better cross-polarized isolation, nominal gain options of -3 dBic and 10 dBic, and SMA mounts. www.pasternack.com

Orbital Insight and Carahsoft partnership

Carahsoft Technology will serve as Orbital Insight's Master Government Aggregator after announcement of partnership between the two. This makes the company's AI-powered geospatial data analytics available to the Public Sector through Carahsoft's reseller partners, and Information Technology Enterprise Solutions – Software 2 (ITES-SW2), NASA Solutions for Enterprise-Wide Procurement (SEWP) V, National Association of State Procurement Officials (NASPO) ValuePoint, National Cooperative Purchasing Alliance (NCPA) and OMNIA Partners contracts. carahsoft.com

Mach9 launches new geospatial production software

Mach9 launched its first product, which leverages AI and computer vision to produce 2D and 3D CAD and GIS engineering deliverables. This product launch comes amidst Mach9's pivot to a software-first business model. www.mach9.io

Planet and ASU to build global solutions

Planet Labs have solidified a Strategic Partnership with Arizona State University (ASU) to facilitate climate action through education and research, workforce development, and a science-first approach toward innovation.

Since 2016, Planet and ASU have collaborated on significant programs including the Planet Incubator Program within ASU's Center for Global

SUBSCRIPTION FORM

YES! I want my **Coordinates**

I would like to subscribe for (tick one)

1 year 2 years 3 years

12 issues

24 issues

36 issues

Rs.1800/US\$140

Rs.3400/US\$200

Rs.4900/US\$300

*

**SUPER
saver**

First name

Last name

Designation

Organization

Address

City Pincode

State Country

Phone

Fax

Email

I enclose cheque no.

drawn on

date towards subscription

charges for Coordinates magazine

in favour of 'Coordinates Media Pvt. Ltd.'

Sign Date

Mail this form with payment to:

Coordinates

A 002, Mansara Apartments

C 9, Vasundhara Enclave

Delhi 110 096, India.

If you'd like an invoice before sending your payment, you may either send us this completed subscription form or send us a request for an invoice at iwant@mycoordinates.org

* Postage and handling charges extra.

MARK YOUR CALENDAR

April 2023

GISTAM 2023

25-27 April

Prague, Czech Republic

<https://gistam.scitevents.org/Home.aspx>

May 2023

International Conference on Geomatics Education

10-12 May 2023

Hong Kong

www.polyu.edu.hk/lsgi/icge22/en

Geo Business 2023

17-18 May

London, UK

www.geobusinessshow.com

9th International Conference on Geomatics and Geospatial Technology

22-25 May 2023

Kuala Lumpur, Malaysia.

<http://ggt2023.uitm.edu.my>

FIG Working Week 2023

28 May - 01 June

Orlando, Florida, USA

www.fig.net/fig2023

June 2023

TransNav 2023

21-23 June

Gdynia, Poland

<https://transnav2023.umg.edu.pl>

July 2023

Esri User Conference

10-14 July, 2023

San Diego, CA, USA

www.esri.com

IGAARS 2023

16 - 21 July

Pasadena, CA, USA

<https://2023.ieeeigarss.org>

September 2023

Commercial UAV Expo

5-7, September 2023

Las Vegas, USA

www.expouav.com

Discovery and Conservation Science, the development of the Allen Coral Atlas, as well as two of the founding partners in the creation of the Carbon Mapper mission. In early 2019, ASU became Planet's first campus-wide university partner, and since then, over 30 peer reviewed journal articles have been published by ASU using Planet products. www.planet.com

Maxar to provide environmental monitoring for Guyana

Maxar Technologies announced that the Guyana Ministry of Natural Resources (MNR) has entered into a three-year contractual agreement with Maxar to provide the nation with environmental monitoring services for both offshore and terrestrial applications. The agreement with Guyana marks Maxar's first Crow's Nest contract in Latin America and the Caribbean and is an important milestone in the application of Crow's Nest to the environmentally critical use case of monitoring offshore petroleum activity. www.maxar.com

RoboSense launches LiDAR solution

RoboSense has announced the launch of its first automotive-grade solid-state LiDAR perception solution for L4 autonomous driving, the RS-Fusion-P6 (P6). The P6 provides precise and intelligent environmental perception capabilities, enabling autonomous vehicles to navigate through complex driving scenarios with ease, helping to reduce costs and increase efficiency, and promoting the rapid implementation of large-scale autonomous driving commercial operations. robosense.cn

FORM IV

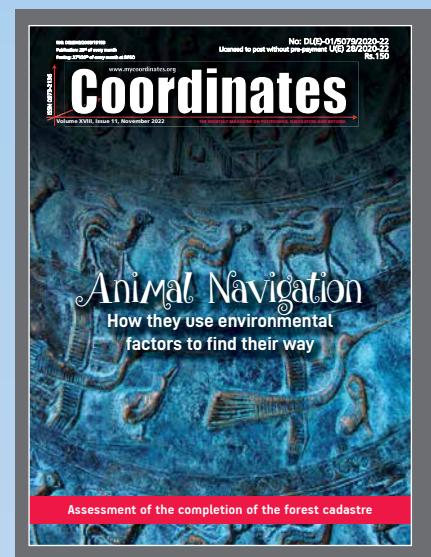
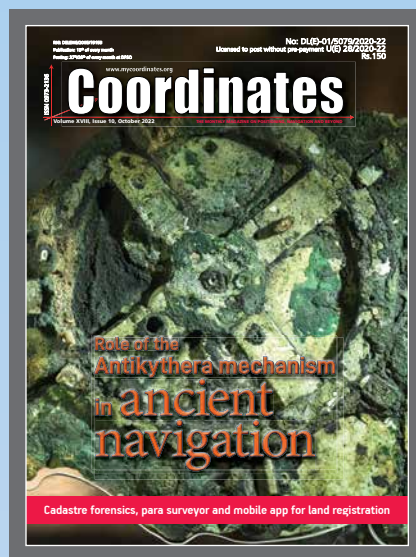
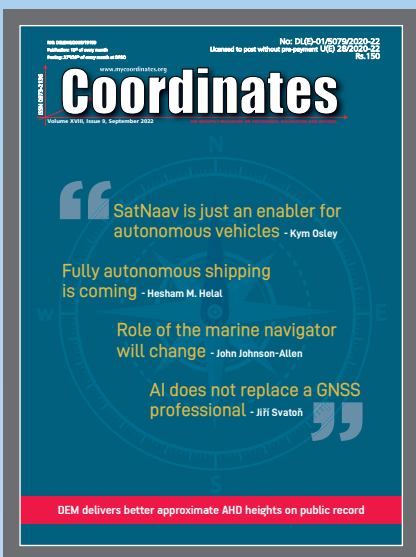
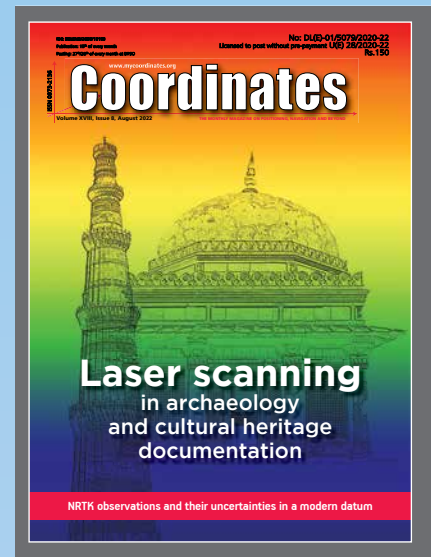
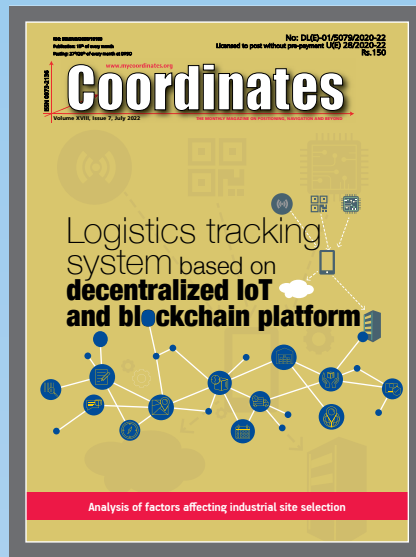
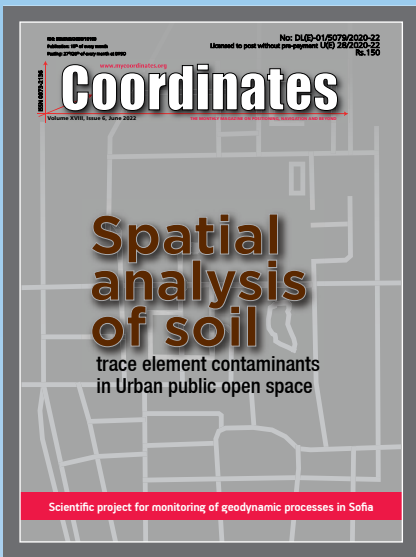
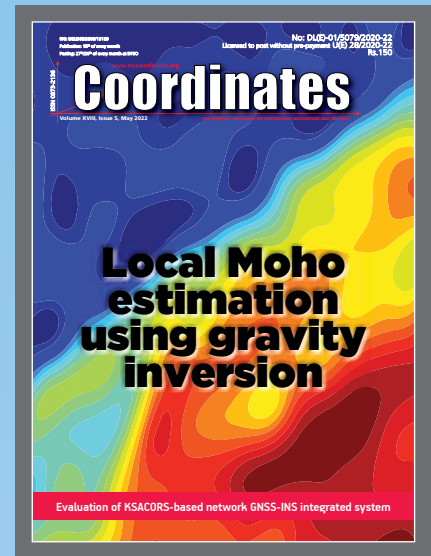
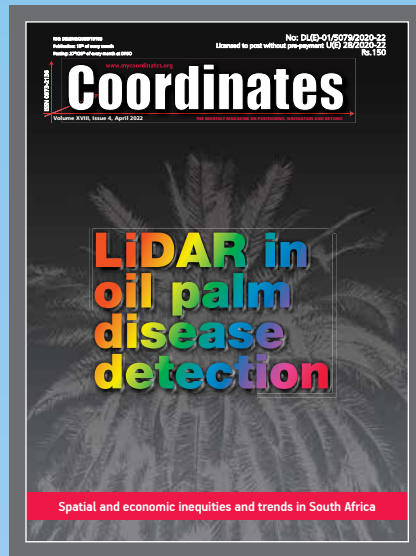
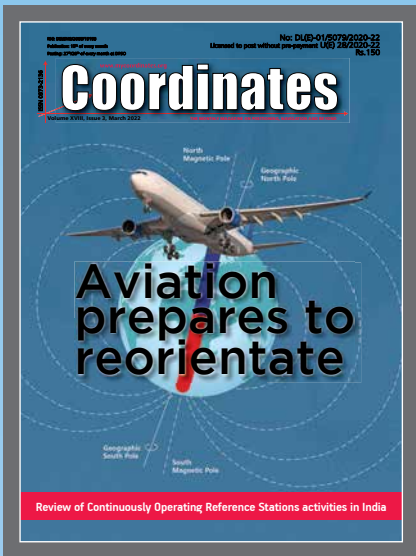
Place of publication: New Delhi
Periodicity: Monthly
Printer's name: Thomson Press
Nationality: Indian
Address: Mathura Road,
Faridabad, India

Publisher's name: Sanjay Malaviya
Nationality: Indian
Address: 499D, Shipra Sun City,
Indrapuram, Gaziabad
Editor's name: Bal Krishna
Nationality: Indian
Address: A 002, Mansara
Apartments, C 9,
Vasundhara Enclave,
Delhi - 110096

I, Sanjay Malaviya, hereby declare that the particulars given above are true to the best of my knowledge and belief.

March 1, 2023

Signature of publisher



“The monthly magazine on Positioning, Navigation and Beyond”
 Download your copy of Coordinates at www.mycoordinates.org



0.05°
ATTITUDE

0.02°
HEADING

1 cm
POSITION

NEW ELLIPSE-D

The Smallest Dual Frequency & Dual Antenna INS/GNSS

- » RTK Centimetric Position
- » Quad Constellations
- » Post-processing Software



Ellipse-D
RTK Dual Antenna



Ellipse-N
RTK Single Antenna



OEM
RTK Best-in-class SWaP-C